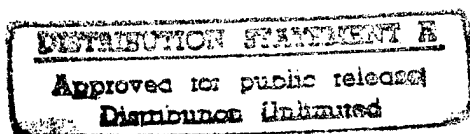




# Comparison of Separation Shock for Explosive and Nonexplosive Release Actuators on a Small Spacecraft Panel

M. H. Lucy and R. D. Buehrle  
*Langley Research Center, Hampton, Virginia*

J. P. Woolley  
*Lockheed Martin, Sunnyvale, California*



December 1996

19970630 098

National Aeronautics and  
Space Administration  
Langley Research Center  
Hampton, Virginia 23681-0001

DTIC QUALITY INSPECTED 1

**COMPARISON OF SEPARATION SHOCK  
FOR  
EXPLOSIVE AND NON-EXPLOSIVE RELEASE ACTUATORS  
ON A  
SMALL SPACECRAFT PANEL**

**TABLE OF CONTENTS**

ABSTRACT.....	1
1.0 SUMMARY.....	1
2.0 INTRODUCTION.....	1
3.0 TEST SETUP AND PROCEDURE.....	2
3.1 Release Mechanisms.....	2
3.2 Test Panel Configurations.....	3
3.2.1 Bare Panel Tests.....	3
3.2.2 Mass Simulator Tests.....	3
3.3 Release Device Mounting.....	3
3.4 Preload.....	3
3.5 Accelerometer Locations and Types.....	3
4.0 DATA ACQUISITION AND PROCESSING.....	4
4.1 Shock Measurements.....	4
4.1.1 Time-Histories.....	4
4.1.2 Shock Response Spectra.....	4
4.2 Impedance Measurements.....	5
5.0 DISCUSSION OF RESULTS.....	5
5.1 Shock Responses.....	6
5.1.1 Mass Loaded Panel Configuration (OEA, Hi-Shear 8mm and, 1/2-inch, ..... G&H and Martin Concept)	6
5.1.1.1 Representative Response Levels.....	6
5.1.1.2 Comparison of Effects of Preload Level for the Martin Concept.....	7
5.1.1.3 Comparison of Levels from Different Release Devices.....	7
5.1.2 Bare Panel Configuration (OEA, Hi-Shear 1/2-inch and G&H Devices).....	7
5.1.2.1 Representative Response Levels.....	8
5.1.2.2 Comparison of Levels from Different Release Devices.....	8
5.1.3 Comparison of SRS Levels with the Bare and Mass Loaded Panel.....	8
5.2 Impedance and Transfer Functions.....	8
6.0 CONCLUSIONS AND RECOMMENDATIONS.....	9
7.0 ACKNOWLEDGMENTS.....	9
TABLE 1 CRSS Radial Panel Development Pyro Shock Tests.....	10
FIGURES.....	11
APPENDIX A, Data Tables A -I Through III.....	36

# COMPARISON OF SEPARATION SHOCK FOR EXPLOSIVE AND NON-EXPLOSIVE RELEASE ACTUATORS ON A SMALL SPACECRAFT PANEL

## ABSTRACT

Functional shock, safety, overall system costs, and emergence of new technologies, have raised concerns regarding continued use of pyrotechnics on spacecraft. NASA Headquarters-Office of Chief Engineer requested Langley Research Center (LaRC) study pyrotechnic alternatives using non-explosive actuators (NEAs), and LaRC participated with Lockheed Martin Missile and Space Co. (LMMSC)-Sunnyvale, CA in objectively evaluating applicability of some NEA mechanisms to reduce small spacecraft and booster separation event shock. Comparative tests were conducted on a structural simulator using five different separation nut mechanisms, consisting of three pyrotechnics from OEA-Aerospace and Hi-Shear Technology and two NEAs from G&H Technology and Lockheed Martin Astronautics (LMA)-Denver, CO. Multiple actuations were performed with preloads up to 7000 pounds, 7000 being the comparison standard. All devices except LMA's NEA rotary flywheel-nut concept were available units with no added provisions to attenuate shock. Accelerometer measurements were recorded, reviewed, processed into Shock Response Spectra (SRS), and comparisons performed. For the standard preload, pyrotechnics produced the most severe and the G&H NEA the least severe functional shock levels. Comparing all results, the LMA concept produced the lowest levels, with preload limited to approximately 4200 pounds. Testing this concept over a range of 3000 to 4200 pounds indicated no effect of preload on shock response levels. This report presents data from these tests and the comparative results.

## 1.0 SUMMARY

Concerns arising from continued use of pyrotechnics on spacecraft led NASA Headquarters-Office of Chief Engineer to request Langley Research Center (LaRC) form a Pyrotechnic Alternatives Investigative Team. In February 1995 LaRC was invited to cooperatively participate with LMMSC in evaluating actuation shock produced by several pyrotechnic and non-pyrotechnic release devices. The tests would objectively investigate application of some non-explosive actuators (NEAs) to reduce small spacecraft and booster separation event shock by demonstrating NEA release mechanisms, comparing resulting levels with those from standard pyrotechnic devices, and evaluating effects of a different test panel mounting arrangement.

Tests were conducted at LMMSC on a structural simulator representing a current small spacecraft panel design--with and without mass loading. Five different release mechanisms were tested in multiple firings with preloads ranging from about 3000 to 7000 pounds, the latter being the comparison standard. With the exception of a LMA rotary flywheel-nut developmental NEA device, hereafter referred to as the Martin concept, all other separation devices were available, off-the-shelf units with no additional provisions to attenuate functional shock.

Accelerometer measurements were made on the panel face and frame, acceleration-time histories reviewed for validity, valid data processed into Shock Response Spectra (SRS), and the SRS data compared. As expected, comparisons for standard preloaded (7000 pound) release mechanisms indicated the most severe levels were produced by the pyrotechnic devices, while the G&H NEA device produced the lowest levels. The Martin concept clearly produced the lowest levels, but its maximum preload capability was limited to approximately 4200 pounds. However, results from testing this developmental device, where the preload range was 3000 to 4200 pounds, indicated there was no systematic effect raising shock levels with preload.

Panel in-plane strain energy release was found to significantly raise the in-plane SRS levels compared to those in the direction normal to the panel face. Normal direction levels were influential at low frequencies, but in-plane levels clearly dominated at frequencies above 600 to 800 Hz. This result was not device dependent, although some spectral differences were noted between the pyrotechnic and NEA devices. Impedance and transfer function data support consistency of the SRS directional response evaluations. This latter data should prove useful in translating these test results to other structures, providing similar data are available on those structures.

## 2.0 INTRODUCTION

Due to concerns arising from continued use of pyrotechnics on spacecraft, NASA Headquarters-Office of Chief Engineer, requested LaRC form a Pyrotechnic Alternatives Investigative Team. Reasons for this request included: high functional (actuation) shock levels; overall system costs; reusability, shrinking volume, weight and power budgets on smaller spacecraft; emergence and availability of new technologies; potentially hazardous nature of the materials involved; and several recent anomalies in which pyrotechnics could be suspect. Because of this activity, in February 1995, LaRC was invited to participate in a cooperative, cost sharing effort with LMMSC to evaluate functional shock produced by several pyrotechnic and non-pyrotechnic release devices. Consequently, LaRC initiated Task 31, "Low-Shock Booster Release

Limited data exist for determining component exposure to shock from payload separation devices on lightweight-rigid structures characteristic of current generation, commercial sized spacecraft. Release devices used on previous spacecraft structures are expected to produce shock levels above those for which many standard components have been qualified. A current LMMSC spacecraft, Commercial Remote Sensing Satellite (CRSS), employs separation devices mounted so a major portion of the strain energy released upon separation is in the mounting plane of some major components. Most current experience is with mounting release devices on external brackets, which convert release motion into transverse bending waves before the shock reaches most components of interest. Together, these situations provided a strong motivation to obtain test data for the LMMSC mounting configuration using current separation devices and prospective devices that promise to produce lower component shock levels. A shock test program was devised and carried out to obtain such data.

The Task's purpose was to objectively investigate application of some NEAs to reduce small spacecraft and booster separation event shock levels. The primary goal was to demonstrate NEA mechanisms for release functions, and determine severity and compare resulting shock levels with those produced by standard pyrotechnic devices. A secondary goal was to evaluate effects of the different release device panel mounting arrangement. LMMSC's initial planning included developing math models, making analytical shock predictions, comparing test results with predictions, and correlating results with the math models. Program resources and schedule precluded development of math models.

The resulting shock test program provided data from five different separation devices (all essentially separation nut designs) mounted as indicated (Figure 1) on a model of the CRSS Radial Panel. This panel was configured with mass simulators representing one of the more heavily loaded CRSS panels. Tests were also performed using three of the release devices on the same panel in a bare configuration (no mass simulators). The standard preload released in the tests was 7000 pounds, as measured by a load cell washer under the restraining bolt head. However, two of the devices tested were incapable of achieving this preload level. One of these, the Martin concept, showed considerable promise for producing low shock levels. To assess its shock level variation with preload, a range of preloads from 3000 to 4200 pounds was used for this device. Shock acceleration response level data were recorded at various points on the panel for each device actuated.

Additional tests were performed to measure release device input mounting impedance and installed accelerometer mounting block transfer functions. Such measurements are intended to aid in extrapolating the included test measurement results to other mounting and structural configurations. A detailed description of the test setup and procedure is provided as a further aid in interpreting test results. One possible method for performing such an extrapolation is described in Reference 1<sup>1</sup> which resulted from work performed on NASA contract NAS5-29452 as reported in Reference 2<sup>2</sup>.

### 3.0 TEST SETUP AND PROCEDURE

#### 3.1 Release Mechanisms

Five different release mechanisms, immediately available from several sources, were tested on a single test panel. Mechanisms ranged from state-of-the-art pyrotechnics (OEA [Ordnance Engineering Associates]-Aerospace 3/8-inch diameter and Hi-Shear Technology Corporation 8mm and 1/2-inch diameter standard separation nuts--figure 2) to NEA designs (G&H Technology, Incorporated and Martin concept rotary flywheel-nut 3/8-inch diameter separation devices--figure 3). To obtain meaningful data, multiple firings of each device were conducted.

With the exception of the Martin concept, all other separation nuts were available, off-the-shelf units with no additional provisions to attenuate actuation shock. The Martin concept (currently under patent disclosure) was an engineering feasibility demonstration unit. Fundamentally it consisted of a housing containing a multi-start, coarse threaded bolt, rotary nut, and locking mechanism. It was fully reusable, required minimal actuation energy, and functioned in less than 50 msec. Exclusive fabrication rights for the Martin concept are held by Starsys Research Corporation of Boulder, CO where the concept, now referred to as the Fast Acting Shockless Separation Nut (FASSN), is undergoing further development as a flight-weight unit. Under their Advanced Release Technologies Satellite (ARTS) II Program, the Naval Research Laboratory, Naval Center for Space Technology, Washington, DC is currently evaluating FASSN in a 1/2-inch diameter size with a preload capability of 10,000 to 13,000 pounds. Eventually Lockheed Martin plans to evaluate a similar device and may investigate a 1-inch diameter sized FASSN in the 50,000 to 70,000 pound preload category.

<sup>1</sup> NASA CR-183480; Shock Prediction Technology: Pyroshock Source Characteristics Study; S.L.Hancock, J.H.Shea, G.R.Dunbar, P.Chao, and A.W.York.

<sup>2</sup> NASA CR-183479; Shock Prediction Technology: Technical Manual; Y.A.Lee, D.R.Crowe, W.Henricks, and D.M.Park.

### **3.2 Test Panel Configurations**

Tests were conducted at LMMSC on a structural simulator (Figure 1) representing a proposed Lockheed Martin Launch Vehicle (LMLV) CRSS Radial Panel--with and without mass loading. This panel was considered representative of a current small spacecraft design. The test unit consisted of a flat 1.5-inch thick honeycomb rectangular panel with overall dimensions of approximately 19-inches by 38-inches. The test unit was suspended by two bungee cords and prevented from excessive swinging by a third bungee attached to the bottom. Y orientation was perpendicular to the panel face, with X and Z in the plane of the panel.

The panel consisted of a honeycomb core, face sheets, and a frame. The honeycomb core was 4.5-pounds per cubic foot aluminum, and the face sheets were 0.032-inch thick 2024-T3 aluminum. The panel was framed by 0.080-inch 6061-T651 aluminum which formed a 1.5-inch wide channel with 1-inch legs. The face sheets were laid over and adhesively bonded to the 1-inch legs. The bottom cut-out (Figure 1) was the release interface site. This cut-out was framed by channel similar to that around the rest of the panel except the legs were 0.125-inch thick. The extension at the bottom of the cut-out frame, through which the release bolt passed, was a minimum of 5/8-inch thick aluminum. Tests were run in a bare panel configuration and in a configuration in which mass simulators were mounted to inserts through the panel face. Table 1 presents detailed conditions of all tests, devices tested, and the preload for each as determined by a load cell washer.

#### **3.2.1 Bare Panel Tests**

Tests were run in the bare panel configuration for the OEA and G&H 3/8-inch, and the Hi-Shear 1/2-inch diameter devices. Due to limited availability of devices, only one test per device was run in the bare panel configuration.

#### **3.2.2 Mass Simulator Tests**

Tests were conducted for all included separation devices with mass simulators attached to the panel. In general, three actuations were conducted for each device. However, the Martin concept was actuated seven times with preloads ranging from 3000 to 4200 pounds. Mass simulators were constructed of aluminum plate, having the same weight and footprint on the panel as the actual component. As shown on Figure 1, three simulators were used: two identical, 30-pound simulators were mounted on opposite sides of the panel; and a third 53-pound simulator was mounted nearer to the release interface.

### **3.3 Release Device Mounting**

Separation system mounting design for this panel (Figure 1) is somewhat unique as the majority of strain energy released upon device actuation is along directions in the plane of the panel. Of particular interest in these tests was the distribution of shock loads among the different directions for this mounting configuration. Such motion excites different modal groups than the more usual, bracket mounted release mechanisms. The latter tends to primarily excite panel bending modes where components are mounted, resulting in the dominant shock levels being oriented normal to the panel's surface.

The release interface was represented by a 1/2-inch thick steel plate, 10-inches square, representing the launch vehicle simulator as shown on Figure 1. When a release device was actuated, this plate fell away thereby producing no secondary contact with the test panel. Separation devices were mounted so the nut and catcher fell away with the steel plate, the bolt staying with the test panel. Additionally, bolts attaching the nut to the plate were loose so the nut separated from the plate by approximately 1/16-inch. Videotape recordings made of each test verified clean separation.

### **3.4 Preload**

The release devices had maximum preload capabilities ranging from about 3000 to 20,000 pounds. A 7000 pound preload was the comparison standard. In this Task, ranges of test parameters were minimized to obtain direct comparisons; however, based on bolt strength, the Hi-Shear 8mm pyrotechnically actuated separation nut was only capable of about 2700 pounds preload. The Martin concept was incapable of the desired preload. To help evaluate effects of preload, a series of tests were performed on the Martin concept in which only preload was varied. The remaining devices were tested at 7000 pounds preload. The load cell washer, from which preload was determined, was located under the bolt head on the panel side of the interface.

### **3.5 Accelerometer Locations and Types**

Data acquisition included 13 accelerometer measurements on the panel's outer frame edge, to which the release device was mounted. Additionally, 23 accelerometer data measurements were obtained on the panel face, where components would usually be mounted. These latter accelerometers were mounted and data recording arranged so that panel instantaneous directional response could be determined. Adequate frequency response up to 10 kHz was available.

The locations of various accelerometer blocks are shown on Figure 1. There were eight pyramid-shaped triaxial blocks and six wedge-shaped biaxial blocks. Each was configured to provide normal (Y) and unambiguous in-plane (X and Z) instantaneous accelerations for the surface on which they were mounted. The X and Z accelerations could be combined to yield an instantaneous in-plane resultant, which should represent the maximum in-plane acceleration amplitude experienced at the measurement location.

Different accelerometers were used on different blocks to accommodate the expected environment. Where the highest levels were expected, Endevco type 7755 accelerometers, with a frequency response of + or - 5 percent from 10 Hz to 10 kHz and a maximum range of 50,000 g, were used on blocks 1,3 and 4. These accelerometers had an 11 kHz mechanical filter to prevent high frequency, high level accelerations from corrupting lower frequency data. Endevco type 2255 accelerometers, with a frequency response of + or - 5 percent from 20 Hz to 20 kHz and a maximum range of 20,000 g, were used on block 2. Endevco type 7250 accelerometers, with a frequency response of + or - 5 percent from 3 Hz to 20 kHz and a maximum range of 5,000 g, were used on the remaining blocks (pyramid blocks 5 through 8 and wedge blocks 9 through 14).

Accelerometers in locations 1 through 8 were mounted in a triaxial configuration on the pyramid-block mounts. The pyramid mounts were geometrically designed to co-locate the three accelerometer sensitive axes at the specimen surface (block mounting face). Locations 9 through 14 were mounted in a biaxial configuration using the wedge-block mounts. The wedge mounts also geometrically positioned the two accelerometers to produce co-incident sensitive axes at the specimen surface.

## **4.0 DATA ACQUISITION AND PROCESSING**

### **4.1 Shock Measurements**

The CRSS panel release mechanism shock measurement data were recorded using LMMSC's acoustic real-time data acquisition system for vibration and acoustic testing. The system is composed of accelerometer transducers, signal conditioning, anti-alias filters, digitizing and storage components. The signal digitization was performed at 50,000 samples per second with a resolution of 14 bits (1 in 16384).

#### **4.1.1 Time-Histories**

Basic shock data were recorded in the form of acceleration-time histories. Accelerometer blocks were shaped so the time phased data could be combined to obtain resultant acceleration-time histories in any direction. Particularly, acceleration-time history in the direction normal to the block mounting surface, and at least one direction in the plane of this surface could be determined for each block. The pyramid block permitted resolution of acceleration into two orthogonal directions in the plane of its mounting surface, as well as into an instantaneous resultant acceleration in that plane.

Response acceleration-time histories were reviewed to determine individual measurement validity. Data determined to be valid was further processed into SRS. SRS were computed using a standard dynamic amplification factor (Q) of 10 (5 percent of critical damping). Data reduction was performed in stages to take advantage of existing LMMSC post-processor software. First, accelerometer responses from each mounting block were vector summed to produce acceleration resultants in the three primary panel axes (X-Y-Z for the pyramid and Y-Z or X-Z for the wedge). These resultants were stored in ASCII data files, one per block-panel axis. Data from positions 1 through 8 were also vector summed to produce the in-plane (X-Z plane) resultants. Finally, the ASCII data were input to the SRS post-processor to produce the SRS output and plot data files.

Typical X-,Z- and Y-direction acceleration-time histories are shown on Figures 4 and 5. These are typical of results obtained from resolving pyramid block data into orthogonal components. Similar results were produced by such resolution of the two-dimensional wedge blocks. Figure 4 is an acceleration-time history taken from a test of the G&H NEA separation nut. Figure 5 is similar data taken from a test of the Martin concept. Exclusive of the maximum levels indicated, the first figure is more typical of separation nut acceleration-time histories (explosive or NEA) in that there is only a single pulse associated with release. Data from the Martin concept, shown in Figure 5, exhibits three distinct pulses, indicative of extended and multiple actions involved in the release process for this mechanism.

#### **4.1.2 Shock Response Spectra**

The ASCII data files were read into the processor, the anti-alias (11.2 kHz) filter transfer function was analytically removed and a six pole, 10 Hz AC coupling was performed. The SRS was generated from 100 to 10,000 Hz with 1/6th-octave filters. Positive, negative and noise floor SRS were computed. Files were also generated containing the time-history and envelope of the SRS.

## 4.2 Impedance Measurements

A series of tests to characterize dynamic behavior of the CRSS panel when subjected to pyrotechnic inputs was performed. These "tap" tests were performed using a Kistler instrumented hammer with an integral, calibrated load cell to tap on a bolt representing the release device bolt. A special hard tip was used to provide significant energy up to 10 kHz. An accelerometer placed on this bolt and the hammer's load cell enabled determination of an input impedance. The same accelerometers and locations as shown in Figure 1 were used throughout the release tests, but the mass simulators were removed. The response of these accelerometers were recorded during the tap tests to determine the transfer function relating their response to a general input excitation. A series of measurements were taken with the 3/8-inch diameter pyrotechnic-attachment point configuration. Then the hole was drilled to accept the 1/2-inch diameter pyrotechnic device, and another series of measurements taken.

The tests were performed by first, attaching a steel block (1.25-inch cube) at the panel's release device attachment point. The block was attached by first a 3/8- and later a 1/2-inch bolt, respectively, for the two series of tests. Excitation was provided by impacting the steel block with the instrumented hammer at approximately 1-second intervals for about 30 seconds. In addition to the accelerometers mounted on pyramid and wedge blocks that were used for the release tests, three accelerometers were mounted as close as possible to the impact point:

- a. A Z-accelerator was mounted at the top of the block-attachment bolt.
- b. An X- and Y-accelerator were mounted on the impact block opposite the impact point (refer to Figure 1 for the axis orientations).

These accelerometers, called "foot" accelerometers, were intended to yield data representing the mounting point impedance for this panel. Similar data for another installation should make the present results transferable.

The acceleration- and force-time histories were acquired by the LMMSC real-time data acquisition system. The data acquisition rate was 30,000 samples per second and 8-pole, 11.2 kHz, Butterworth, low-pass (anti-alias) filters were used. The impact levels were nominally 1500 pounds but varied between approximately 800 and 1900 pounds. Data analysis was performed with the signal analysis processor. The procedure was:

A peak detection system was used on the force-time histories to determine when impacts occurred. Exactly 2048 points were selected around each impact. Each time-history was inspected to assure there was a pre-trigger of at least 256 points and that there was only a single impact within the range of sample points. Response data from up to ten of the responses was retrieved for all "acceptable" time windows.

Transfer functions between responses and force input were calculated for each impact. These transfer functions were then averaged (using ten averages for the "3/8-inch bolt" test and at least seven averages for the "1/2-inch bolt" test).

The 1/6th-octave impedance was calculated from the transfer functions by:

1. Calculating the acceleration impulse function via inverse Fast Fourier Transform (FFT).
2. Subtracting off the average offset (AC coupling).
3. Multiplying by 386.4 to convert from a "g" calibration to inches/second/second.
4. Integrating to obtain the velocity impulse function.
5. Calculating the velocity transfer function by forward FFT.
6. Calculating the impedance by complex inversion of the velocity transfer function.

Determination of the 1/6th-octave impedance spectrum was completed by averaging the magnitude of the impedance-spectral components over each 1/6th-octave band. The same 1/6th-octave center frequencies were used for these calculations as for the SRS calculations.

## 5.0 DISCUSSION OF RESULTS

Overall measures of SRS produced by the devices were derived from the data and compared for accelerometers located on the panel face. Comparisons indicated the most severe levels were produced by the OEA device, followed by the Hi-Shear 1/2-inch diameter device. Of the devices capable of 7000 pound preload, the G&H NEA device produced the lowest levels. In these tests the Martin concept clearly produced the lowest levels, but its maximum preload capability was limited. Of the devices tested, LMMSC selected the Hi-Shear 1/2-inch diameter separation nut for further consideration. A comparison of results from the Martin concept for several preloads indicated there was no systematic effect of rising preload causing an increase in shock levels over the range tested. Such a result may eventually break down at some higher level of preload.

In-plane strain energy release was found to significantly raise the shock environment in-plane SRS levels compared to the normal direction levels. It was still found that the normal direction levels were influential at low frequencies, but in-plane levels were clearly dominant in the higher frequencies (above 600 to 800 Hz). This result was not device dependent, although some spectral differences can be noted between the pyrotechnic devices and NEAs. The SRS generally showed an increase with frequency, with only levels and local details varying with device. The panel's dynamic properties probably provide the dominant aspect to determining spectral shapes with the devices all providing broad band excitation, differing primarily in level only.

Impedance and transfer function data taken support the consistency of the SRS directional response evaluations. This data should prove useful in translating the test results contained herein to other structures, providing similar data are available on those structures. Comparative data used in this report are tabulated in Appendix A.

## 5.1 Shock Responses

SRS were determined for five different separation devices with the CRSS panel in the mass loaded configuration and for three different devices with the panel in the bare (unloaded) configuration. Data were resolved into normal (Y-axis) and in-plane (X- and Z-axis) as well as in-plane instantaneous resultant magnitude, before the SRS were calculated. The SRS were computed for each orthogonal axis and in-plane resultant, where such data were available, using the standard Q of 10. SRS data were subjected to statistical analysis using various groupings to obtain comparisons for the differences between devices and test condition effects.

Although data were taken and reduced to SRS form on the frame, only data from the face sheets were used in the analyses. It was anticipated that shock propagation in this panel, with the type of mounting used for the separation devices, would have been rather complex. The frame data were taken to enable the study of shock propagation for the panel in the event these complexities actually appeared. The test results did not indicate that such studies were warranted or necessary, so they were not performed. Only the non-frame, flat panel data are treated herein. These data represent the environment of panel mounted components.

### 5.1.1 Mass Loaded Panel Configuration (OEA, Hi-Shear 8mm and 1/2-inch, G&H and Martin Concept)

Data from all five separation devices were taken for the test panel configured with mass simulators. At least three tests were performed with each device for this panel configuration. Twenty-three accelerometer channels on the panel face were recorded for each test. The standard preload for these tests was 7000 pounds, as indicated by the load cell instrumentation. Two of the devices, the Hi-Shear 8mm device and Martin concept, were not capable of the standard preload. They were loaded to the maximum permissible preload, which was about 2700 pounds for the Hi-Shear 8mm device; and the Martin concept was tested over a range of preloads from 3000 to 4200 pounds, as indicated in Table 1. Assimilation of this mass of data into an interpretable form was the first order of the analysis process. A statistical approach was used for this purpose.

#### 5.1.1.1 Representative Response Levels

Data from any one grouping of measurements was assumed to behave as a log-normal random variable. Various axis groupings were constructed and log-normal statistical properties of these groups were compiled and compared. The groups were: acceleration normal to the panel surface (Y-axis, designated as nfy); orthogonal in-plane (X- and Z-axes, designated as nfxz); in-plane resultant (of X and Z components, designated as nfp); and combined normal and in-plane resultant levels. In computing the statistical properties, no segregation by location on the panel face was included. Nomenclature used includes; nf (no frame), and i or ip (in-plane). Figures 6 (a) through (e) show the comparisons of data groupings 95th percentile levels for each device and preload:

- (a) OEA 3/8-inch diameter pyrotechnic separation nut, 7000 pound preload.
- (b) Hi-Shear 1/2-inch diameter pyrotechnic separation nut, 7000 pound preload.
- (c) G&H 3/8-inch diameter NEA separation nut, 7000 pound preload.
- (d) Hi-Shear 8mm diameter pyrotechnic separation nut, 2700 pound preload.
- (e) Martin 3/8-inch diameter concept, 4000 and 4200 pound combined preload.

Figures 7 (a) through (e) show the same sequence of device results, but compare the maximum measured level in each grouping.

In both sets of above figures, it may be seen that the combined normal and in-plane resultant levels serve as a reasonable indicator of an upper bound level. The upper bound level is always this combination for the maximum measured levels of

Figures 7. This must be true because the in-plane resultant is greater than or equal to the X- or Z-direction maxima and the combined maximum bears the same relation to the normal and in-plane directions.

If the reader seeks differences in the directional SRS levels, it may be observed that the normal direction is somewhat more influential in the lower frequencies and the in-plane motion dominates the higher frequencies. It is suggested by the impedance measurements, discussed later, that one might expect that panel modes associated with bending waves, which involve out-of-plane motion, come to bear at lower frequencies than the shear and longitudinal wave modes. The reader is cautioned that a resonant phenomenon is not involved here, but when the transient motion produced by the release is spectrally resolved, the natural modes of the system will indicate pronounced motion in their frequency bands.

A few instances were noted where the X-Z direction maximum measured level appeared to exceed the in-plane resultant level. These were found to be instances where there had been a zero shift in the accelerometer calibration during the test. This shift was not apparent for the X- or Z- measurements alone, whereas it was for the in-plane measurement. The data had been eliminated from consideration in the latter and not the former and thereby caused the faulty indication. Inspection of the time-histories of the original data confirmed in all cases that the data were faulty when there was a difficulty of this nature.

Figures 8 (a) through (e) show the relation between the arithmetic mean, the log mean, the 95th percentile and the maximum measured levels for the same sequence of devices. The difference between the log mean and the 95th percentile is indicative of the standard deviation for the data. These data, the standard deviation, sample size and Gumbel Factor (a correction for statistical errors due to small sample size) are presented in tabular form in Appendix A, Table A-1, (a) through (e), for the same sequence of devices.

There is close correspondence between the maximum measured and 95th percentile levels. It may be seen from these figures that the maximum measured level is the upper bound of the 95th percentile at all but a few frequency ranges of relatively narrow extent. Further, exceedances in these frequency ranges are of relatively small extent. These facts indicate there is little data scatter. Since data were collected from the entire panel face, this indication reveals there is little spatial variation of the shock levels over the panel face.

#### 5.1.1.2 Comparison of Effects of Preload Level for the Martin Concept

The Martin 3/8-inch diameter NEA concept was incapable of achieving the standard preload. It was tested over a range from 3000 to 4200 pounds. To assess effects of preload on results, these measurements are compared with one another. Combined normal and in-plane resultant levels are used as the basis for this comparison. Statistical features of these measurements are given in Appendix A, Table A-1, (e) through (i), for:

- (e) Combined 4200 and 4000 pound preload
- (f) 4200 pound preload
- (g) 4000 pound preload
- (h) 3500 pound preload
- (i) 3000 pound preload

The 95th percentile and maximum levels are shown in Figures 9 (a) and (b), respectively. The reader should note there is no clear trend associated with preload magnitude, as maximum measured SRS levels for 3000 pound are as great as those for the 4200 pound preload. Interpretation of the 95th percentile data is somewhat more difficult due to the small sample size producing more erratic indications.

#### 5.1.1.3 Comparison of Levels from Different Release Devices

The SRS 95th percentile and maximum levels are compared for all devices as measured with the maximum preload achieved for that device. These are shown in Figures 10 (a) and (b), respectively. The ordering of levels for the different devices is the same for both the 95th percentile and maximum measured levels. The order from higher to lower levels is: OEA; Hi-Shear 1/2-inch; Hi-Shear 8mm; G&H; and the Martin concept. The Martin concept produced levels significantly lower than the others; however, its greatest preload was only 4200 pounds as compared to 7000 pounds for the OEA, Hi-Shear 1/2-inch and G&H devices. Such a difference in preloads could make a significant difference in the shock levels produced, although its variation over the range tested did not indicate a strong dependence on this parameter.

#### 5.1.2 Bare Panel Configuration (OEA, Hi-Shear 1/2-inch and G&H devices)

Tests were performed using OEA, Hi-Shear 1/2-inch and G&H devices at a preload of 7000 pounds with the test panel devoid of mass simulators. Due to limited availability of release devices, it was possible to perform only one test for each

OEA and Hi-Shear 1/2-inch device with the panel in this configuration; however, three tests were performed with the G&H device. A similar procedure was followed for evaluating data from the bare panel tests as was done for the panel with mass simulators.

#### 5.1.2.1 Representative Response Levels

SRS acceleration levels measured on the panel face were grouped in the same axis directions as previously done for the mass simulator data. As before, these groups were subjected to statistical analysis. The 95th percentile data are compared in Figures 11, and Figures 12 for the maximum measured levels with data for the individual devices presented separately in the (a), (b) and (c) versions of these Figures, as follows:

- (a) OEA 3/8-inch diameter pyrotechnic separation nut.
- (b) Hi-Shear 1/2-inch diameter pyrotechnic separation nut.
- (c) G&H 3/8-inch diameter NEA separation nut.

The combined normal and in-plane directions grouping is again considered to best represent the levels produced by each device. However, results are not as clear as before because of the significantly smaller sample sizes in the measurements.

Figures 13 (a) through (c) show the relation between the arithmetic mean, log mean, 95th percentile and maximum measured levels for the same sequence of devices in the bare panel configuration. The difference between the log mean and 95th percentile is indicative of the standard deviation for the data. These data, the standard deviation, sample size and Gumbel Factor are presented in tabular form in Appendix A, Table A-II, (a) through (c), for the same sequence of devices.

Because of the small number of measurements, the 95th percentile levels are frequently greater than maximum measured levels for this series of tests of the OEA and Hi-Shear 1/2-inch devices. This is not the case for the G&H device, since three tests were performed with it in the bare panel configuration.

#### 5.1.2.2 Comparison of Levels from Different Release Devices

SRS acceleration levels from the three devices were compared by means of results from the combined normal and in-plane resultant measurements. Figure 14 (a) and (b) show comparisons between their 95th percentile and maximum measured levels, respectively. The relative levels, as indicated by either the 95th percentile or maximum measured SRS accelerations, indicate the highest output from the OEA device, followed by the Hi-Shear 1/2-inch diameter and G&H device, respectively. However, there appears little difference between the last two devices for these bare panel tests as compared to their relative levels for the panel with mass simulators (refer to Figures 9). The paucity of measurements for the Hi-Shear device in the bare panel configuration is probably a major factor in this apparent difference. It is likely that both the OEA and Hi-Shear device levels are inaccurately represented by the small sample size. Such likelihood is reinforced by the results obtained by comparing the bare and mass loaded panel SRS levels produced by these devices.

#### 5.1.3 Comparison of SRS Levels with the Bare and Mass Loaded Panel

Data representative of the SRS acceleration levels produced by the three devices that were tested on both the bare and mass loaded panel were compared. Figure 15 (a) and (b) show the 95th percentile and maximum measured levels, respectively, for the OEA, G&H and Hi-Shear 1/2-inch devices. This is a replot of data previously presented for each.

The reader may note for the first two devices, there are large frequency bands in which levels for the mass loaded panel exceed those for the bare panel. One is tempted to conjecture by referring to Figure 1, that all accelerometers used in compiling the statistics are in positions that are unshielded by the mass simulators. Furthermore, they may well be the recipient of energy reflected from these simulator bodies, and one might expect higher response levels to be produced. However, data for the G&H device follow the accepted behavior, and indicate the bare panel levels consistently exceed those for the mass loaded panel, as physical reasoning would lead one to expect. Recall that data for the G&H device represent a statistical sample which includes three test actuations of the device for each configuration. The mass loaded data for the OEA and Hi-Shear devices also represent data from three actuations, but the bare panel levels represent data from only one actuation of each. This is an indication that relative levels of the bare and mass loaded panels are not of the same confidence level in representing the expected results from these two devices, whereas, those for the G&H device are.

## 5.2 Impedance and Transfer Functions

Impedance data were calculated for the "foot" accelerometers mounted near the separation device for the test performed with the 3/8-inch bolt. Data from the 1/2-inch bolt test were not as good (the hammer hits and resulting data were erratic), so they have not been reduced to 1/6th-octave results.

The 1/6th-octave "foot" impedances for the three orthogonal directions resulting from excitation in these X-, Z- and Y-directions are shown in Figures 16, 17 and 18, respectively. The plotted data are also tabulated in Appendix A, Table A-III (a) through (c). The first two of these directions lies in the plane of the panel, while the Y-direction is normal to this plane. The general shapes of the impedance curves are similar for the X- and Z-direction excitations and responses, being consistent with no modes associated with motion in these directions below about 600 Hz. The Y-direction excitation impedances exhibit a character indicating modes associated with motion in this direction (probably bending) beginning in the neighborhood of 300 Hz. As was mentioned in describing the SRS results, the Y- (normal) direction of motion seemed to have the greater influence in the low frequencies and the in-plane motion seemed to dominate the higher frequencies.

The "foot" data are intended to represent the mounting point impedance for this panel. Similar data for another installation should enable estimation of the shock input energy obtained in these tests to that of the other installation, given proper dynamic models. The transfer function data for other test panel accelerometer blocks will be useful in constructing and validating such models.

## 6.0 CONCLUSIONS AND RECOMMENDATIONS

SRS results for accelerations on the face sheets, where components are mounted, were combined into axis groups and subjected to statistical analysis. It was found that variation of level over the panel face was relatively small, as indicated in the small standard deviation from the statistical analysis. Differences between normal and in-plane resultant levels were also small although some spectral differences were noted and are described below. A combination of these directional levels was found to fairly represent behavior of the individual devices, although there would be little qualitative difference noted in picking any of the groupings to represent a device.

Overall measures of shock levels (SRS's) produced by the devices were derived from the data and compared for accelerometers located on the panel face. These comparisons indicated the most severe levels were produced by the OEA device, followed by the Hi-Shear 1/2-inch diameter nut. Of the devices capable of 7000 pound preload, the G&H NEA device produced the lowest levels. The Martin concept clearly produced the lowest levels in the test series, but its maximum preload capability was only 4200 pounds.

A comparison of results from the Martin concept for preloads, from 3000 to 4200 pounds, indicated there was no systematic effect raising shock levels with preload for this device over the range tested. However, it is expected that such a result may break down at some higher level of preload or it may be only due to the small amount of data used.

In-plane strain energy release was found to significantly raise the in-plane SRS levels of the shock environment compared to the normal direction levels. It was still found that normal direction levels were influential at low frequencies, but in-plane levels were clearly dominant in the higher frequencies (above 600 to 800 Hz). This result is not device dependent, although some spectral differences can be noted between the pyrotechnic and NEA devices. The SRS trends showed an increase in level with frequency. The dynamic properties of the test panel probably provide the dominant aspect determining the spectral shapes with the devices all producing broad band excitation, differing primarily in level only.

Impedance and transfer function data taken support the consistency of SRS directional response evaluations. They are indicative of the presence of low frequency bending waves (beginning at about 300 Hz) and onset of shear and dilatation waves at the higher frequencies (600 to 800 Hz). This data should also prove useful in translating these test results to other structures, providing similar data are available on those structures.

Data used for comparison purposes in the report are tabulated in Appendix A which represent reduced test data.

## 7.0 ACKNOWLEDGMENTS

This effort was principally performed under Contract NAS1-19241, Task 31, at LMMSC by James P. Woolley, and the LaRC Task Monitor was Melvin H. Lucy, assisted by Ralph D. Buehrle. The point-of-contact (POC) and device provider for the Hi-Shear 8mm pyrotechnic separation nuts was Richard G. Webster. The POCs, device providers and refurbishers for the G&H NEA stored mechanical energy separation nut were John Bielinski and Wayne Powell. The Martin concept was supplied by Bill Nygren from the LAM-Denver Division. The authors express their gratitude to several individuals who contributed to the successful outcome of this program. Special thanks are due LMMSC's Messrs. Strether Smith and William Hollowell for their aid in data acquisition, analysis and post processing, and for their contributions to those report sections. LMMSC's Messrs. Myron Leigh and David Kreuger, who operated the data acquisition system and conducted the test operations, respectively, are responsible for the excellent quality of the data obtained from these tests. Finally, the coordination efforts of Messrs. Mike Otvos and Marc Gronet of LMMSC who set the stage for a seamless effort by the several organizations involved.

**Table 1 CRSS Radial Panel Development Pyro Shock Tests**

Run No.	Test No.	Type	Time/Date	Data File	Preload	Mass Sim	Video No.	Data Table
1	1	3/8 G&H	10:38 27-Mar	L858E01	7000	Yes	3	A-1 (c)
2	2	3/8 G&H	13:21 27-Mar	L858E02	7000	Yes	4	
3	3	3/8 G&H	14:15 27-Mar	L858E03	7000	Yes	5	
4	4	3/8 G&H	15:40 27-Mar	L858E04	7000		6	A-2 (c)
5	5	3/8 G&H	16:49 27-Mar	L858E05	7000		7	
6*		3/8 G&H	18:49 27-Mar		7000		8	
7	6	3/8 G&H	18:56 27-Mar	L858E06	7000		9	A-1 (d)
8	7	8mm HiS	14:59 28-Mar	L858E07	2440	Yes	10	
9	8	8mm HiS	10:30 31-Mar	L858E08	2670	Yes	11	
10	9	8mm HiS	14:40 31-Mar	L858E09	2600	Yes	12	A-1 (a)
11	10	3/8 OEA	14:23 03-Apr	L858E10	7000	Yes	13	
12	11	3/8 OEA	10:54 12-Apr	L858E11	7000	Yes	14	
13	12	3/8 OEA	13:30 12-Apr	L858E12	7000	Yes	15	A-2 (a)
14	13	3/8 OEA	11:20 13-Apr	L858E13	7000		16	
15**		1/2 HiS	15:00 17-Apr		7000		1	
16	14	1/2 HiS	09:38 18-Apr	L858E14	7000		18	A-2 (b)
17	15	1/2 HiS	14:00 18-Apr	L858E15	7000	Yes	19	A-1 (b)
18	16	1/2 HiS	10:24 19-Apr	L858E16	7000	Yes	20	
19	17	1/2 HiS	13:44 19-Apr	L858E17	7000	Yes	21	
20***		3/8 Martin	15:00 19-Apr		2700	Yes	22	A-1 (j) & (k)
21	M1	3/8 Martin	10:23 20-Apr	L858M01	3000	Yes	23	
22	M2	3/8 Martin	11:30 20-Apr	L858M02	3000	Yes	24	
23	M3	3/8 Martin	12:39 20-Apr	L858M03	3000	Yes	25	
24	M4	3/8 Martin	13:13 20-Apr	L858M04	3500	Yes	26	A-1 (e), A-1 (j) & (k)
25	M5	3/8 Martin	13:40 20-Apr	L858M05	4000	Yes	27	
26	M6	3/8 Martin	14:00 20-Apr	L858M06	4000	Yes	28	
27	M7	3/8 Martin	14:28 20-Apr	L858M07	4200	Yes	29	A-3 (a)
	F1	X- Dir Tap						
	F2	Z- Dir Tap						
	F3	Y- Dir Tap						A-3 (c)

\* Wire came loose on firing system - no release, no accl data retained.

\*\* Bolt Bottomed-out in sep nut - squib fired, no release, no accl data retained.

\*\*\* Preliminary release, no accl data recorded.

Note: 1) Because of inaccuracies of load washer, all preload values are approximate.

2) Impedance Test File Names: L858HAM1 thru HAM9. L858HAM4 thru HAM6 are retests of L858HAM1 thru HAM3.

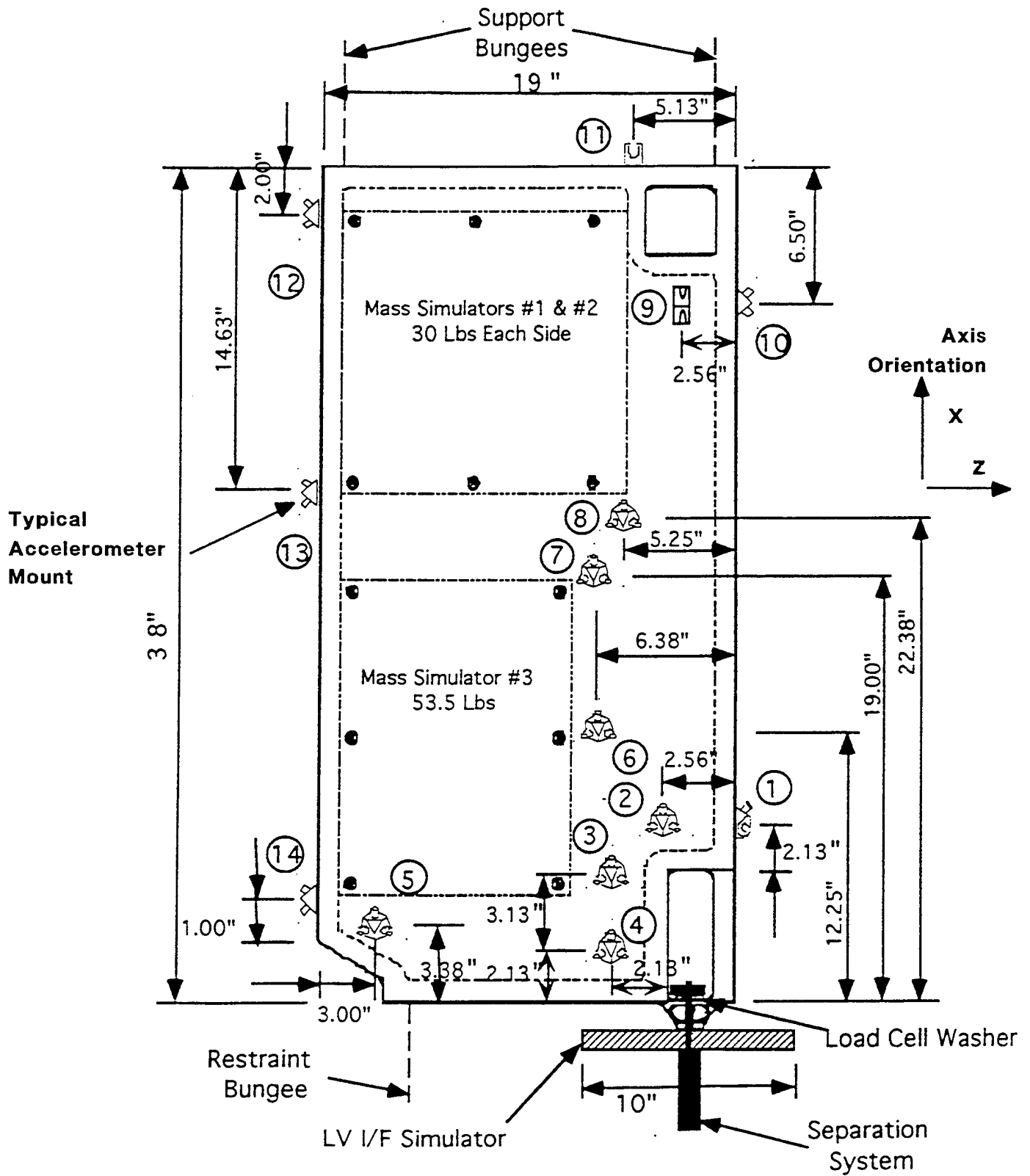


Figure 2. Test Panel with Masses and Accelerometer Block Locations.

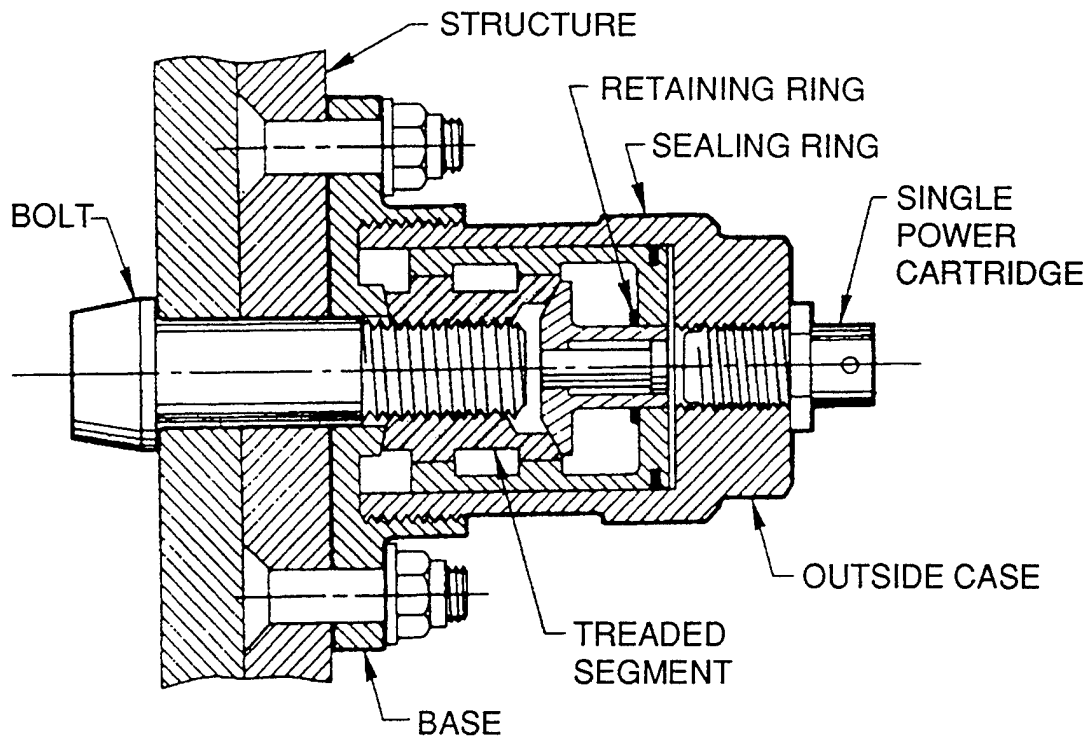
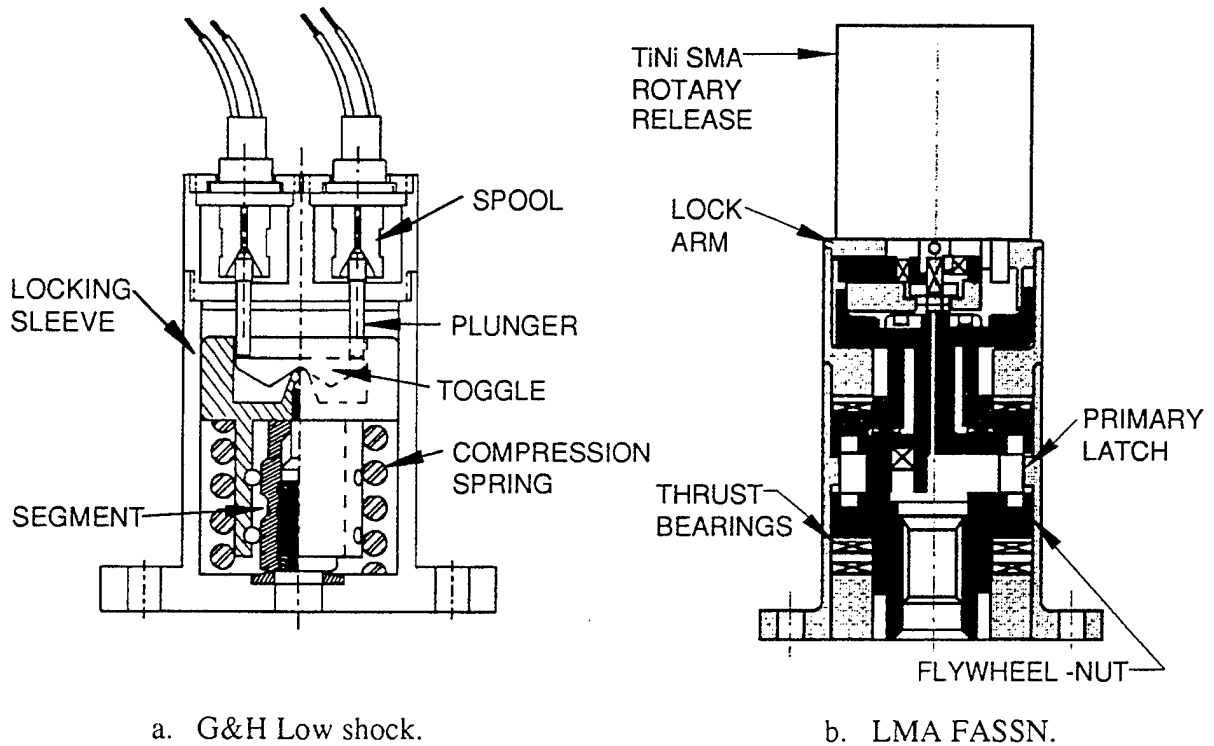


Figure 2. Typical Pyrotechnic Separation Nut (Hi-Shear Depicted).



a. G&H Low shock.

b. LMA FASSN.

Figure 3. Non-Explosive Actuated Separation Devices.

CRSS Dev. PNL PYRO SHOCK #3  
 GNH 3/8" NON-EXPLOSIVE  
 TIME RANGE: 6.86 TO 7.01 Seconds

PLOT MADE ON  
 31-DEC-95 AT 15:21  
 TEST PERFORMED  
 27-MAR-95 AT 14:12

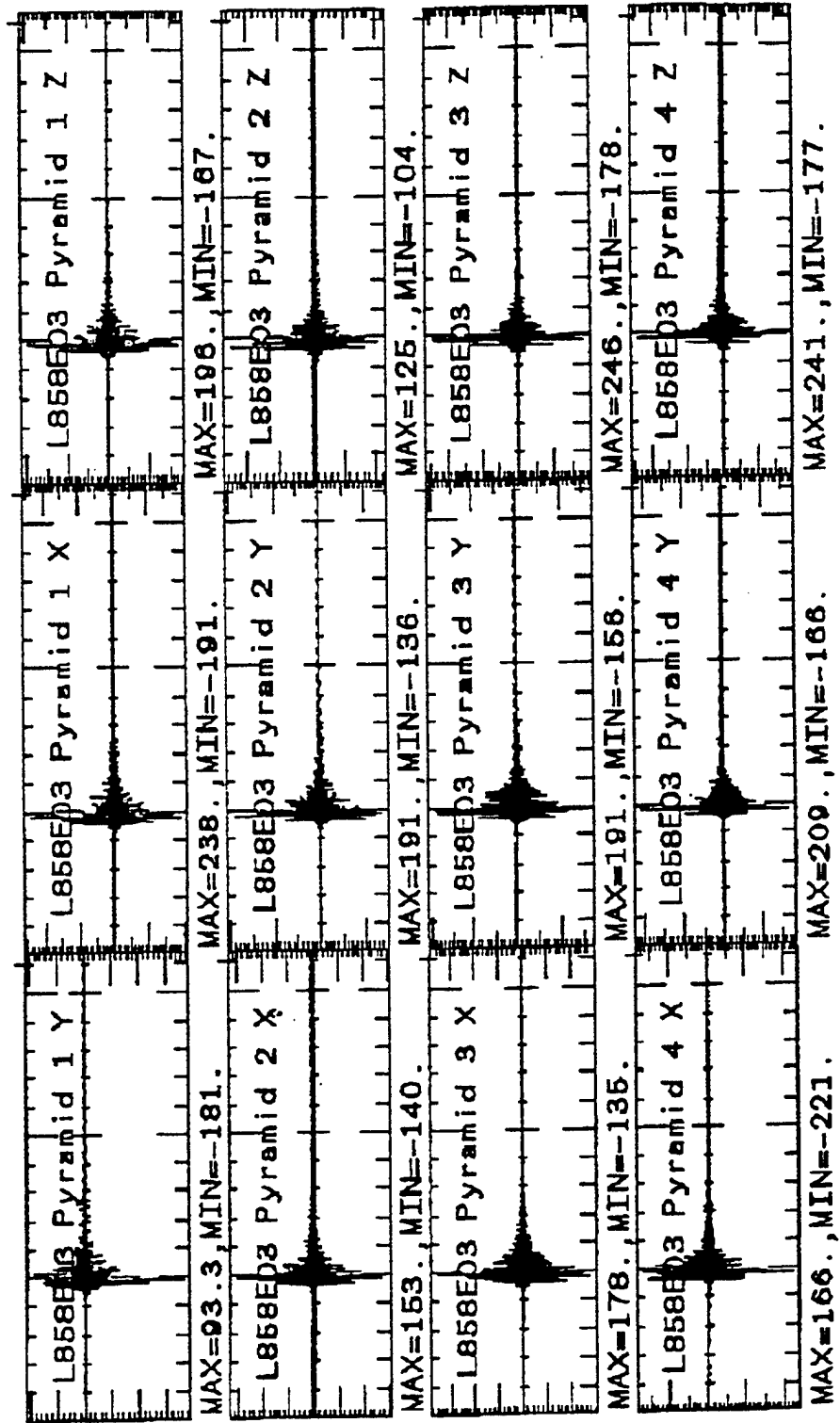


Figure 4. Typical X-, Y-, and Z-Direction Acceleration Time Histories from G&H Device.

CRSS DEV. PNL PYRO SHOCK TEST  
MARTIN ELECT. SEP NUT, TEST #7  
TIME RANGE: 3.37 TO 3.70 Seconds

PLOT MADE ON  
25-APR-95 AT 16:26  
TEST PERFORMED  
20-APR-95 AT 14:51

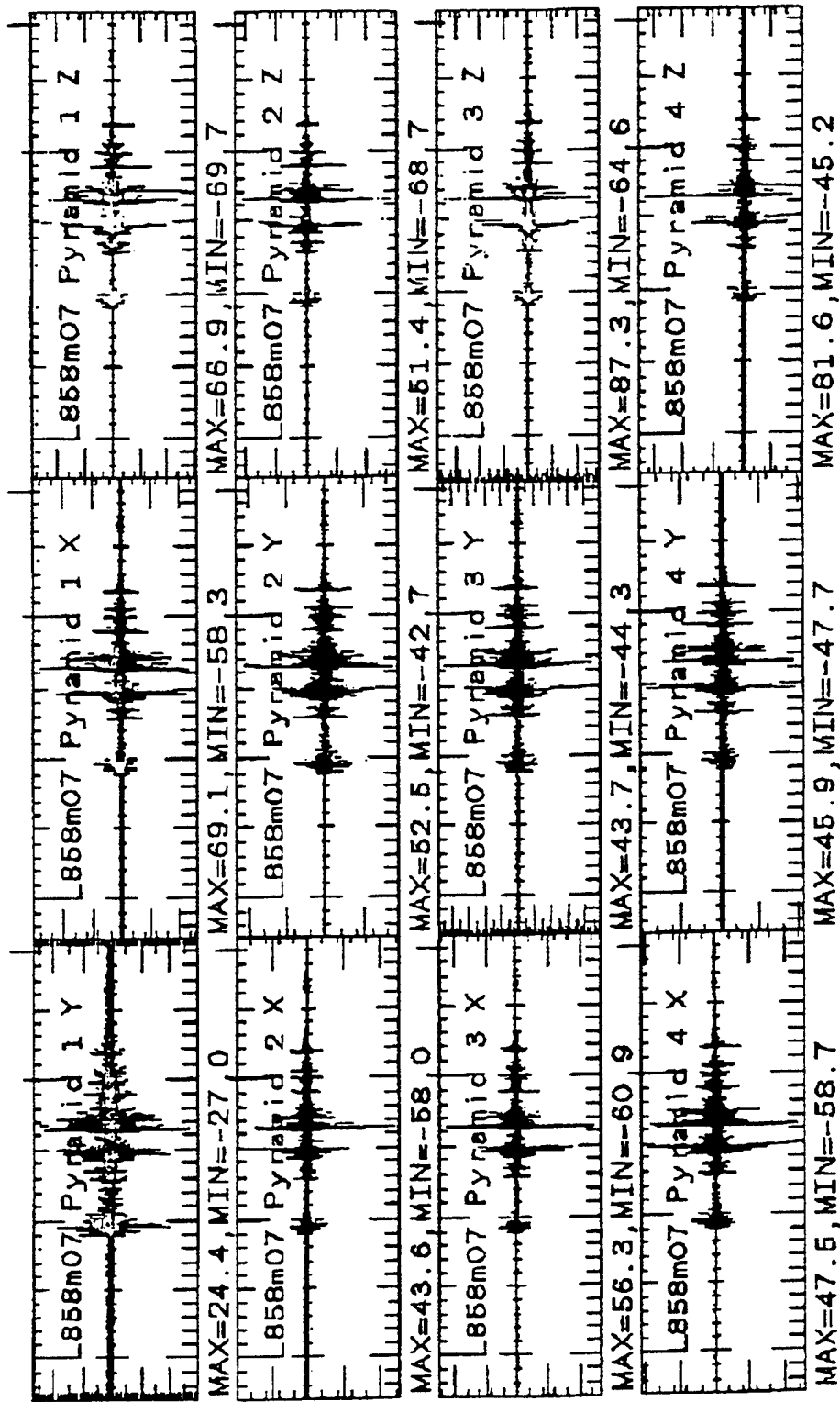
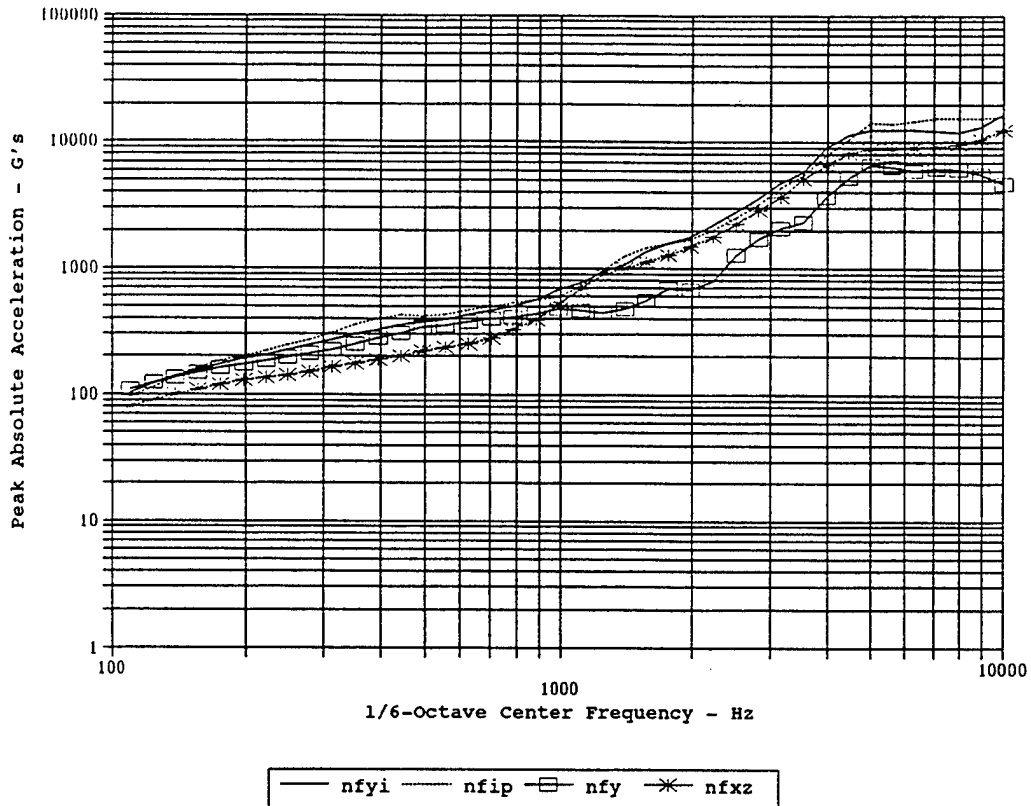
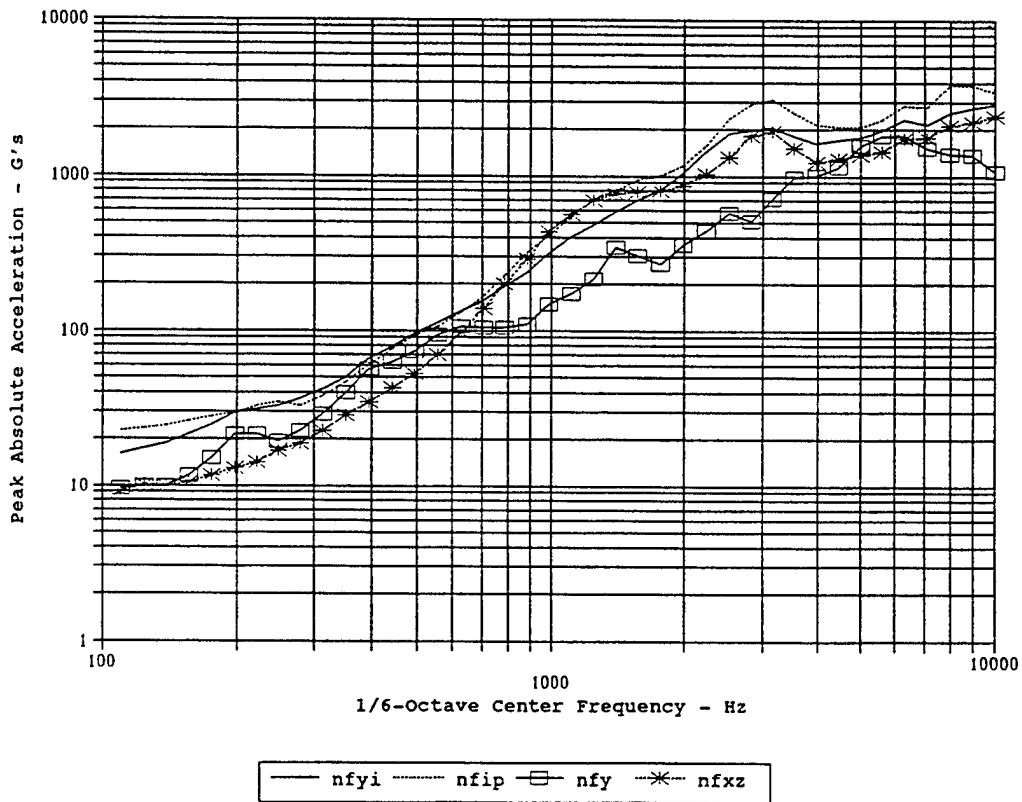


Figure 5. Typical X-, Y-, and Z-Direction Acceleration Time Histories from Martin Device.



**Figure 6(a). OEA 3/8", with Masses, 7000 lb., Various Axis Groupings, SRS (Q=10), 95th Percentile Levels.**



**Figure 6(b). HiS 1/2", with Masses, 7000 lb., Various Axis Groupings, SRS (Q=10), 95th Percentile Levels.**

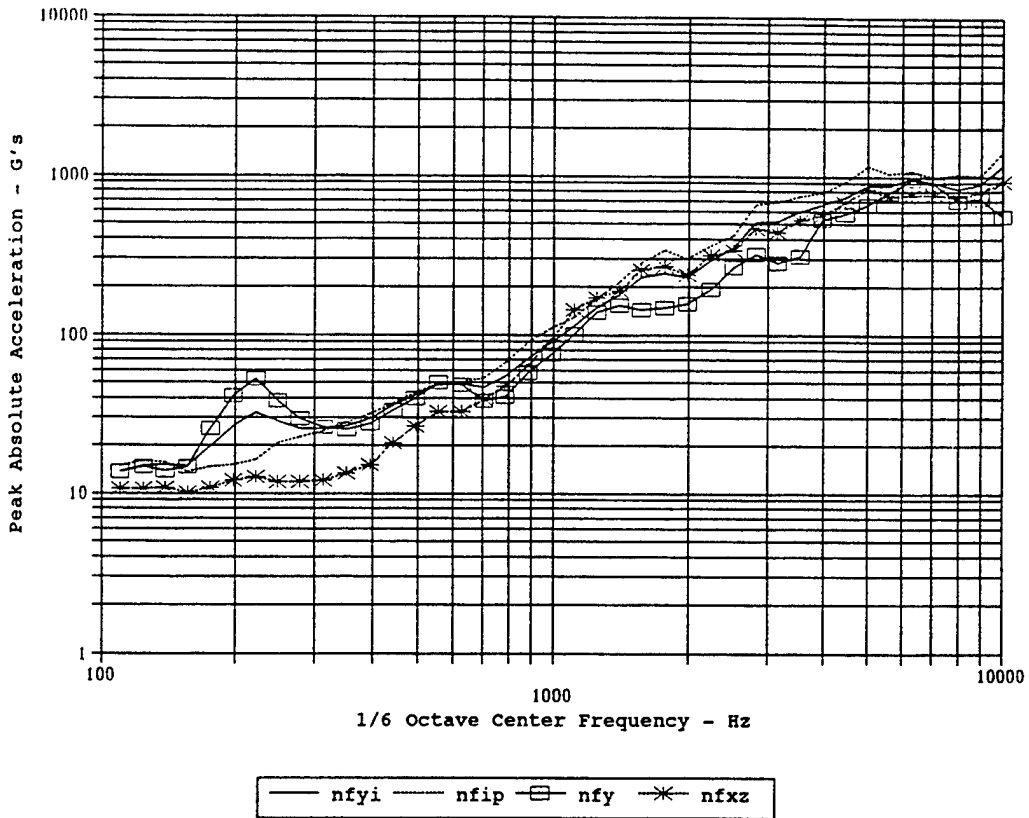


**Figure 6(c). G&H 3/8", with Masses, 7000 lb., Various Axis Groupings, SRS (Q=10), 95th Percentile Levels.**

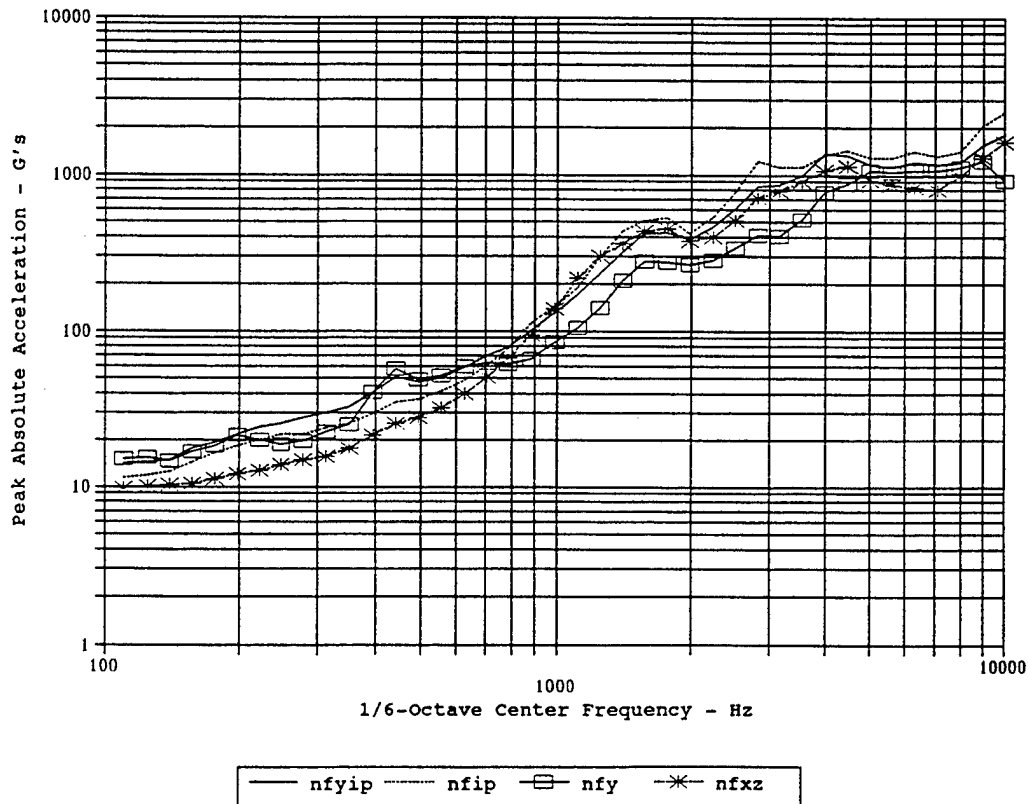
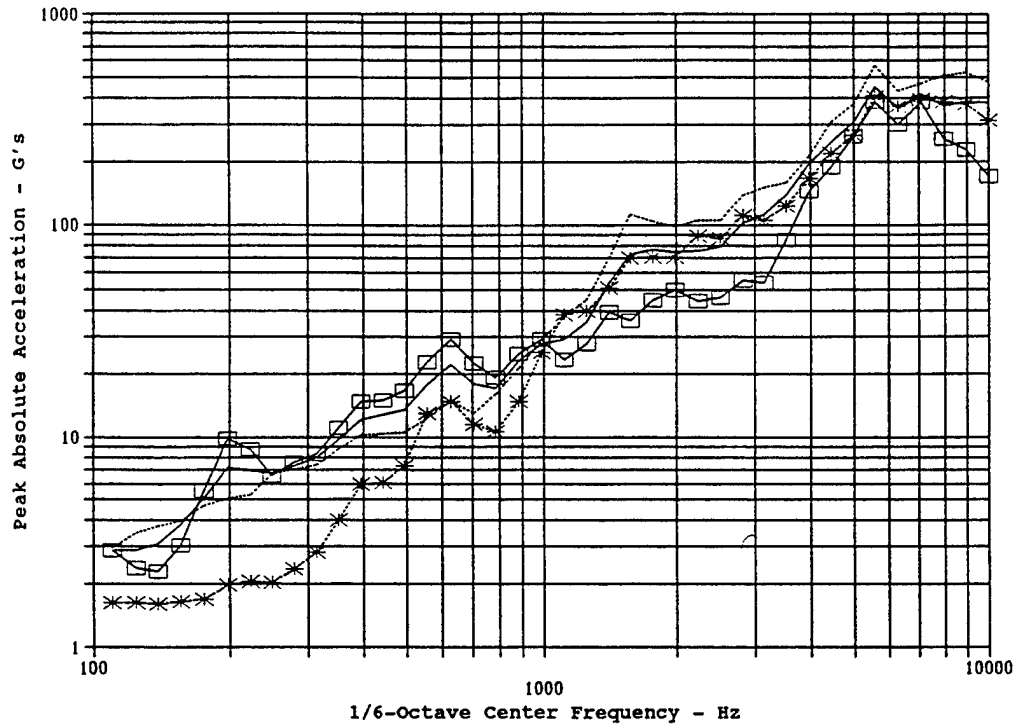


**Figure 6(d). HiS 8 mm, with Masses, 2700 lb., Various Axis Groupings, SRS (Q=10), 95th Percentile Levels.**



— yi4a — ip4a —□— y4a —\*— xz4a

**Figure 6(e). LM 3/8", with Masses, Combined 4000 & 4200 lb., Various Axis Groupings, SRS (Q=10), 95th Percentile Levels.**

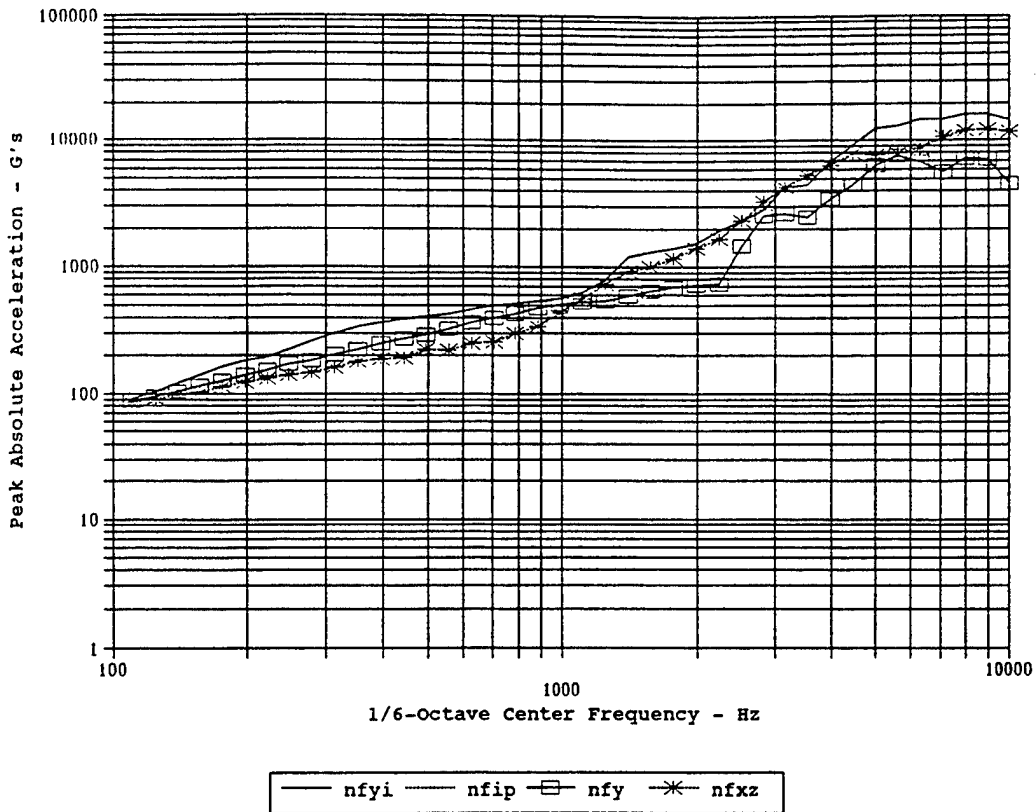


**Figure 7(a). OEA 3/8", with Masses, 7000 lb., Various Axis Groupings, SRS (Q=10), Maximum Measured Levels.**

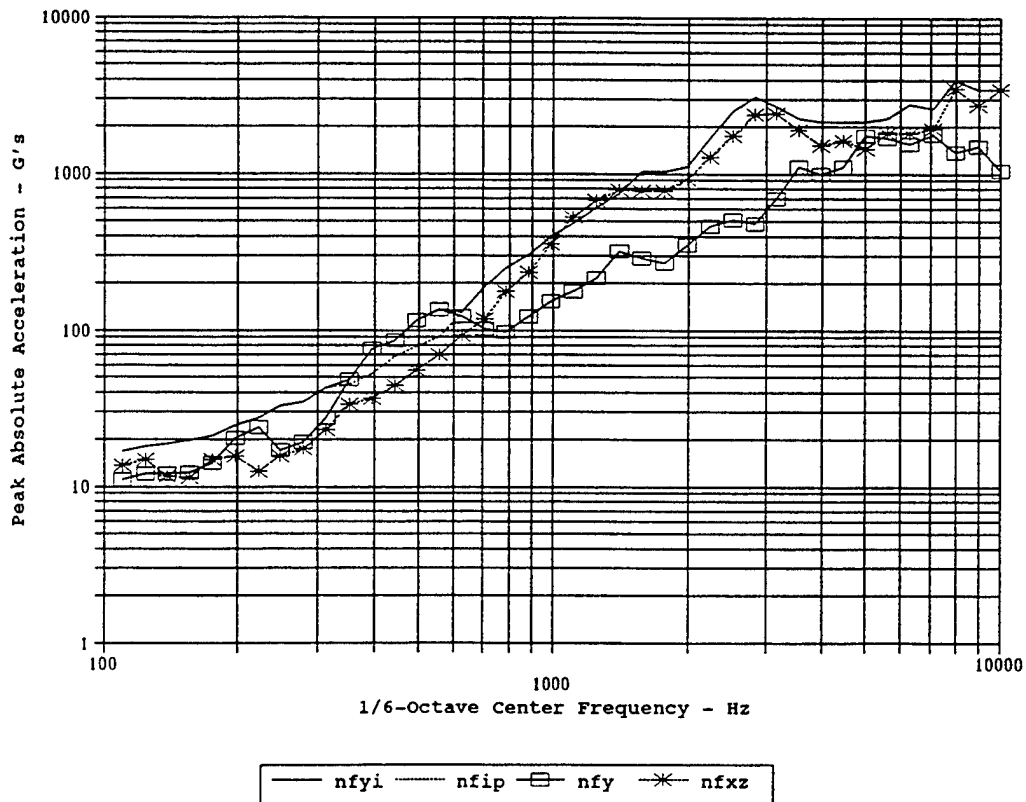
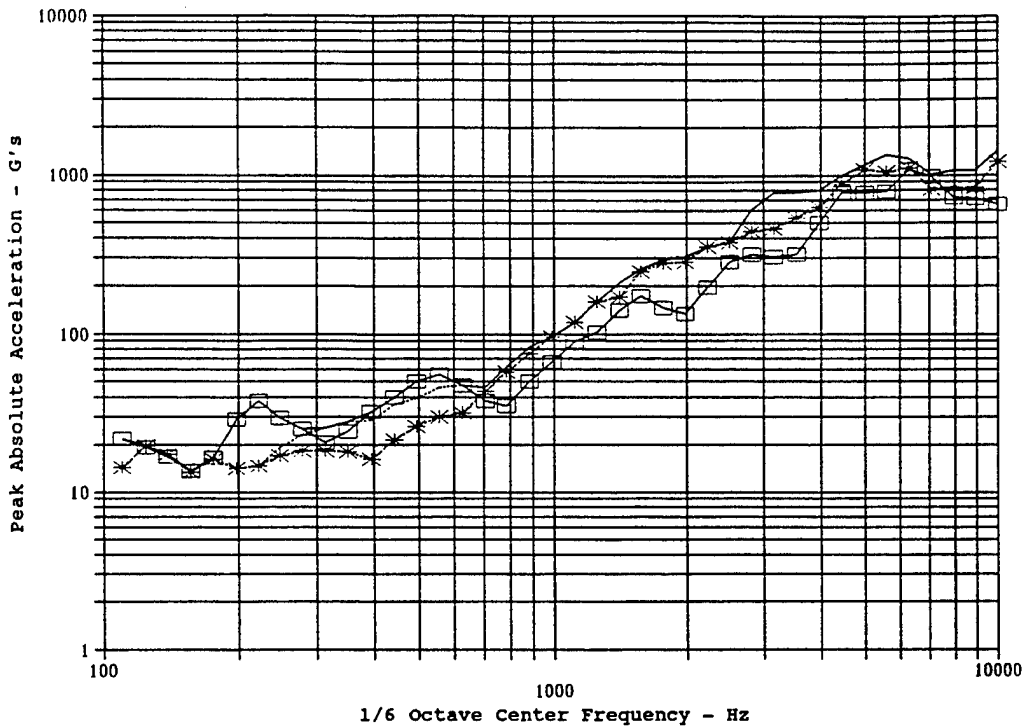
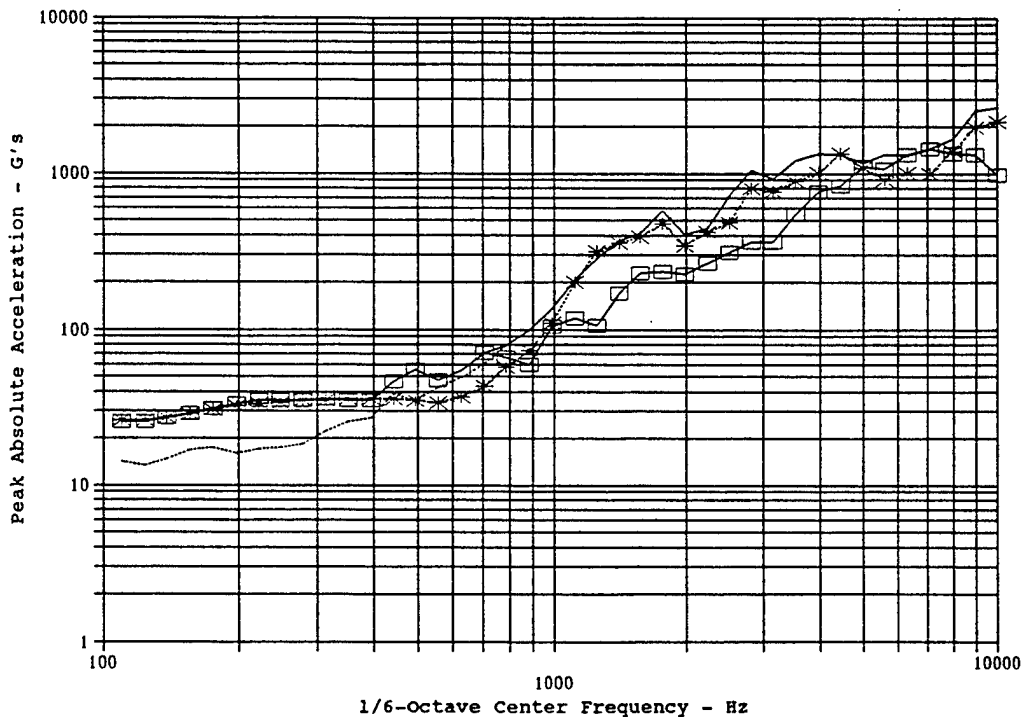


**Figure 7(b). HiS 1/2", with Masses, 7000 lb., Various Axis Groupings, SRS (Q=10), Maximum Measured Levels.**



— nfyi — nfip —□— nfy \* nfxz

**Figure 7(c). G&H 3/8", with Masses, 7000 lb., Various Axis Groupings, SRS (Q=10), Maximum Measured Levels.**



— nfyip — nfip —□— nfy \* nfxz

**Figure 7(d). HiS 8 mm, with Masses, 2700 lb., Various Axis Groupings, SRS (Q=10), Maximum Measured Levels.**

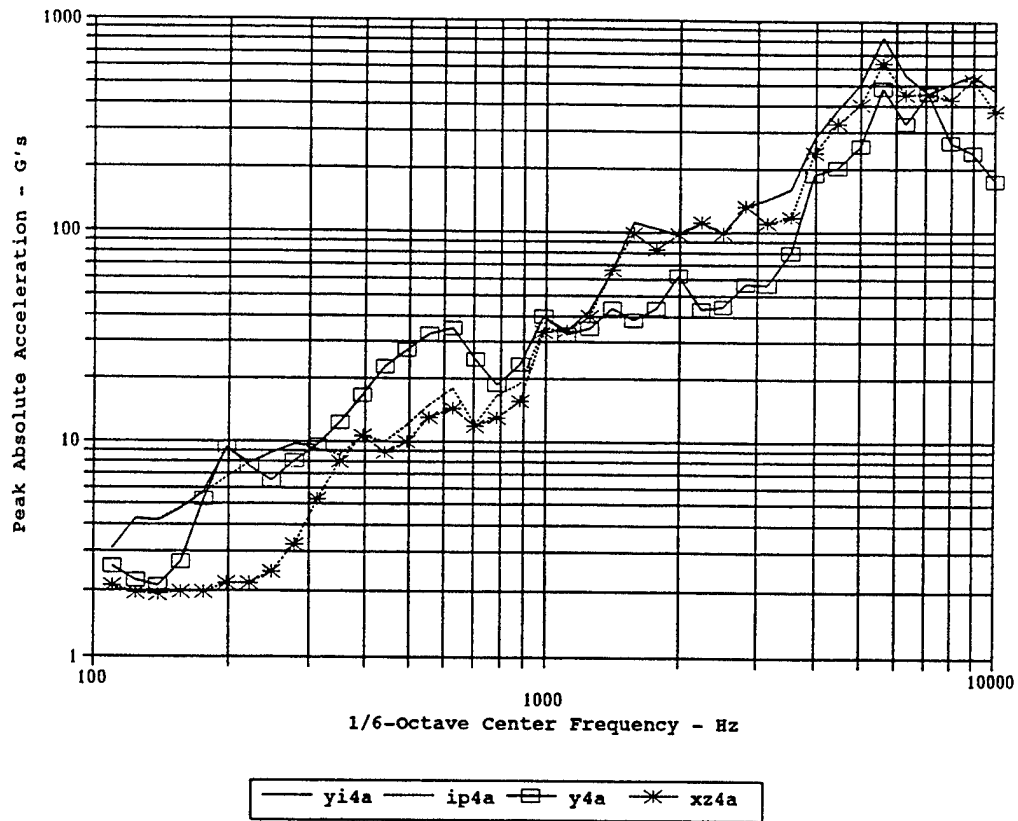
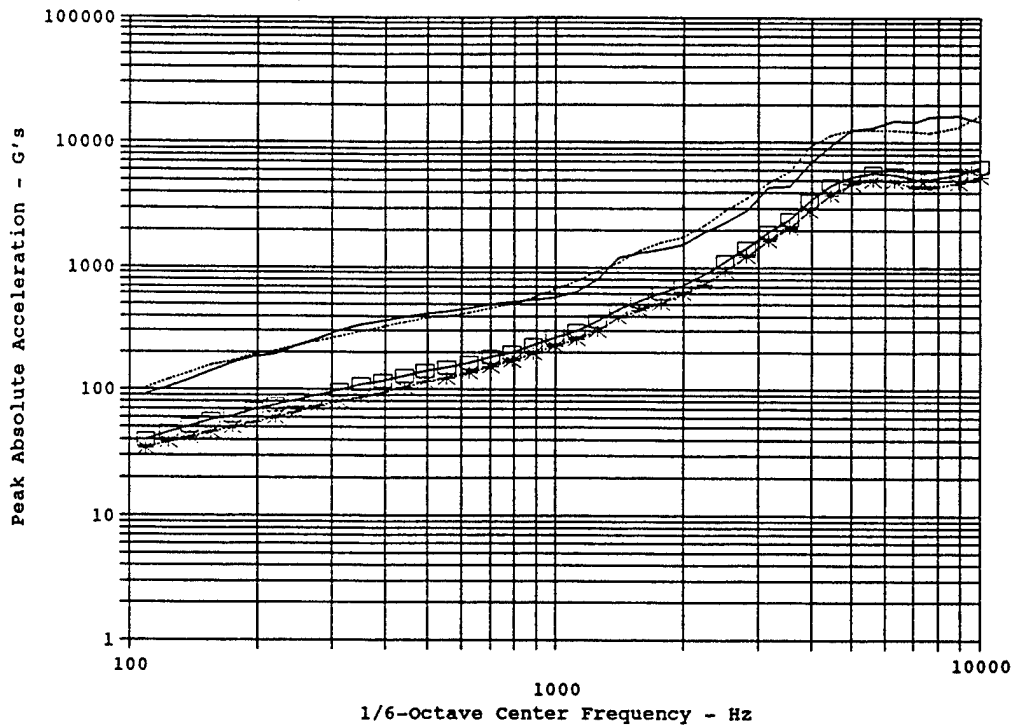
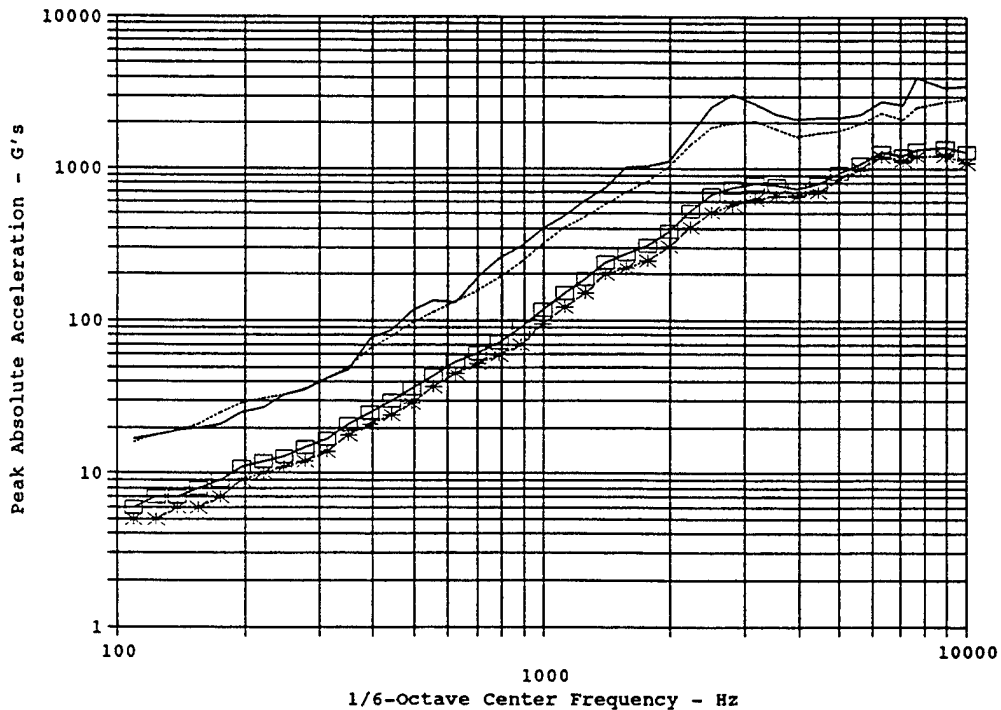


**Figure 7(e). LM 3/8", with Masses, Combined 4000 & 4200 lb., Various Axis Groupings, SRS (Q=10), Maximum Measured Levels.**



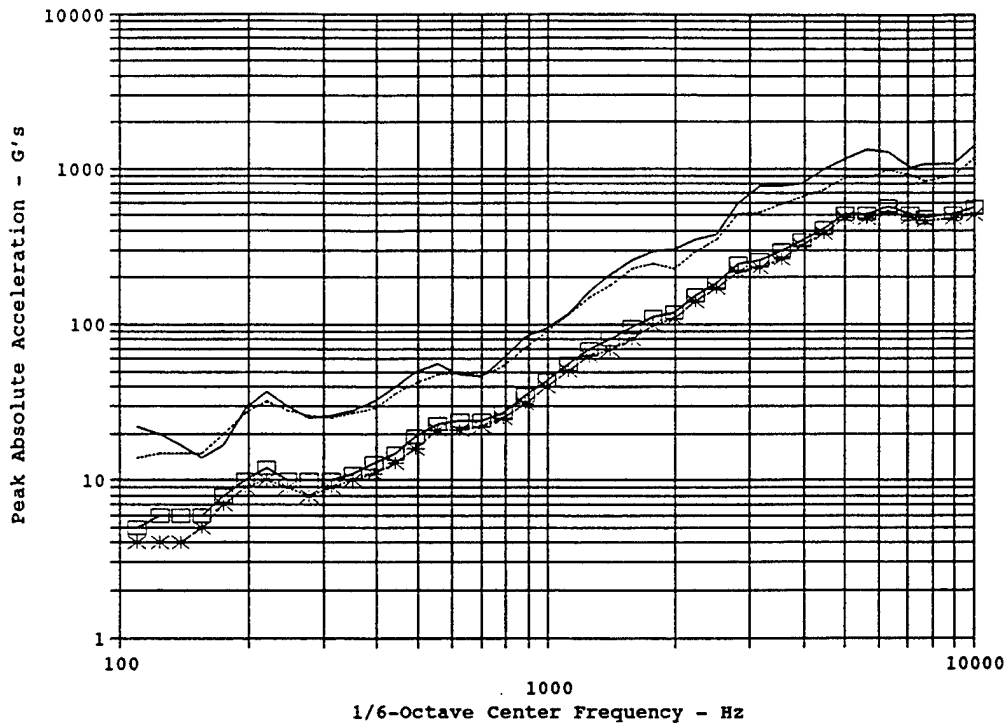
— Max nfyi      - - - 95th% nfyi      □ Arith Mean nfyi      \* Log Mean nfyi

**Figure 8(a). OEA 3/8", with Masses, 7000 lb., Combined Normal & In-Plane Resultant, SRS (Q=10), Log-Normal Statistical Features.**



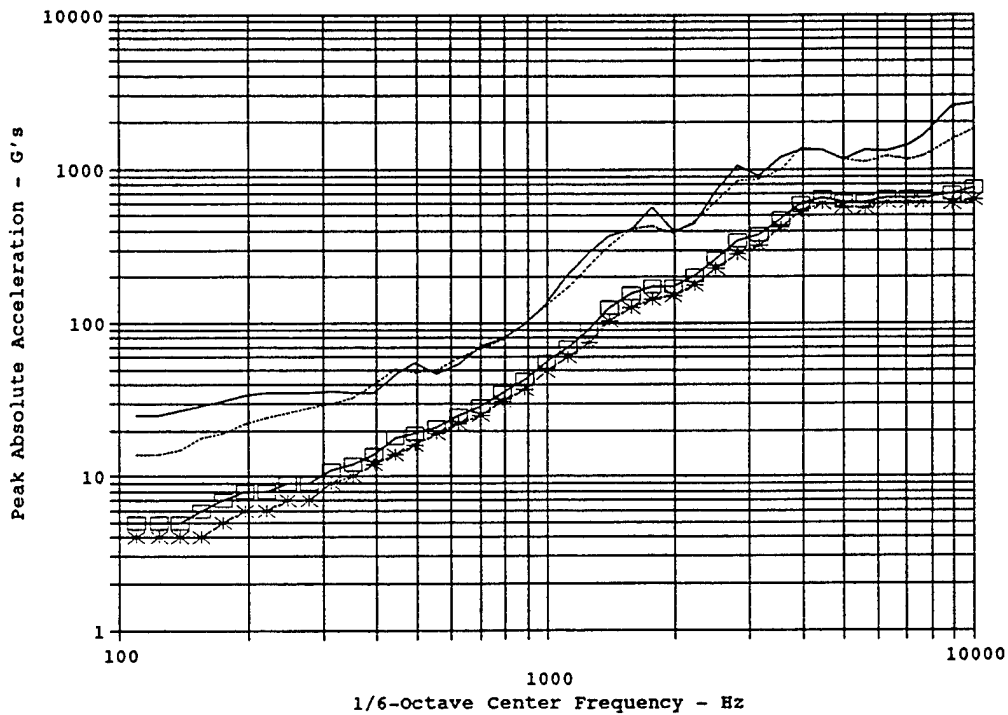
— Max nfyi      - - - 95th% nfyi      □ Arith Mean nfyi      \* Log Mean nfyi

**Figure 8(b). HiS 1/2", with Masses, 7000 lb., Combined Normal & In-Plane Resultant, SRS (Q=10), Log-Normal Statistical Features.**



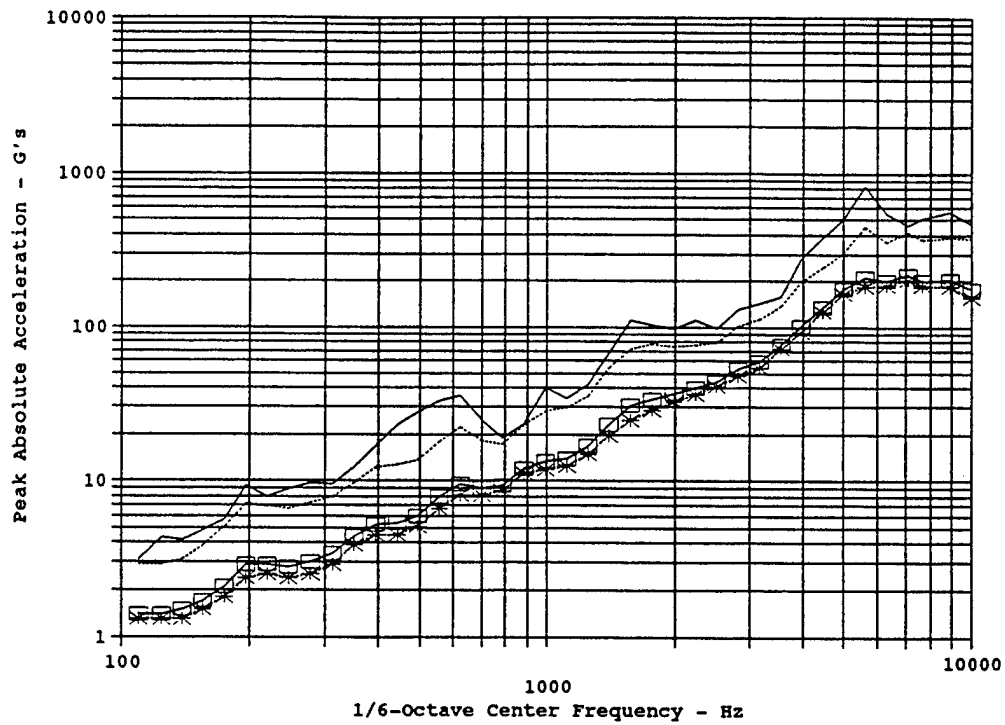
— Max nfyi      - - - 95th% nfyi      □ Arith Mean nfyi      \* Log Mean nfyi

**Figure 8(c). G&H 3/8", with Masses, 7000 lb., Combined Normal & In-Plane Resultant, SRS (Q=10), Log-Normal Statistical Features.**



— Max nfyip      - - - 95th% nfyip      □ Arith Mean nfyip      \* Log Mean nfyip

**Figure 8(d). HiS 8 mm, with Masses, 2700 lb., Combined Normal & In-Plane Resultant, SRS (Q=10), Log-Normal Statistical Features.**



Max yi4a    
  95th% yi4a    
  Arith Mean yi4a    
  \* Log Mean yi4a

**Figure 8(e). LM 3/8", with Masses, Combined 4000 & 4200 lb., Combined Normal & In-Plane Resultant, SRS (Q=10), Log-Normal Statistical Features.**

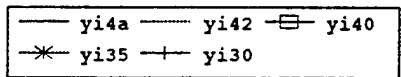
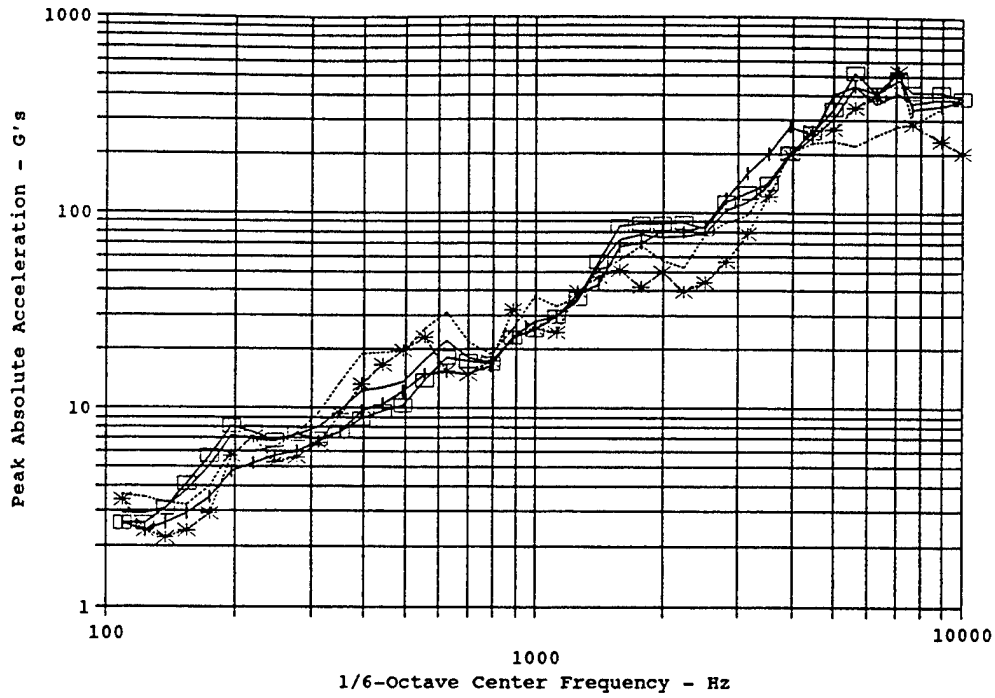


**Figure 9(a). LM 3/8", with Masses, Preload Comparison, Combined Normal & In-Plane Resultant, SRS (Q=10), 95th Percentile Levels.**

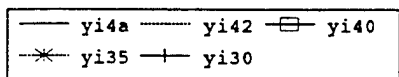
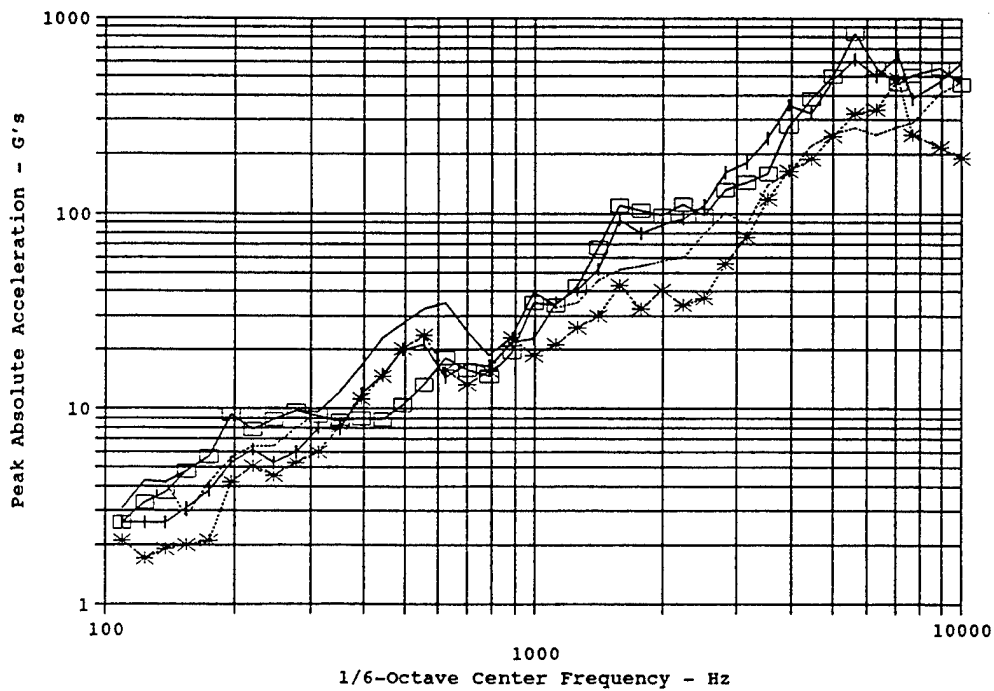


**Figure 9(b). LM 3/8", with Masses, Preload Comparison, Combined Normal & In-Plane Resultant, SRS (Q=10), Maximum Measured Levels.**

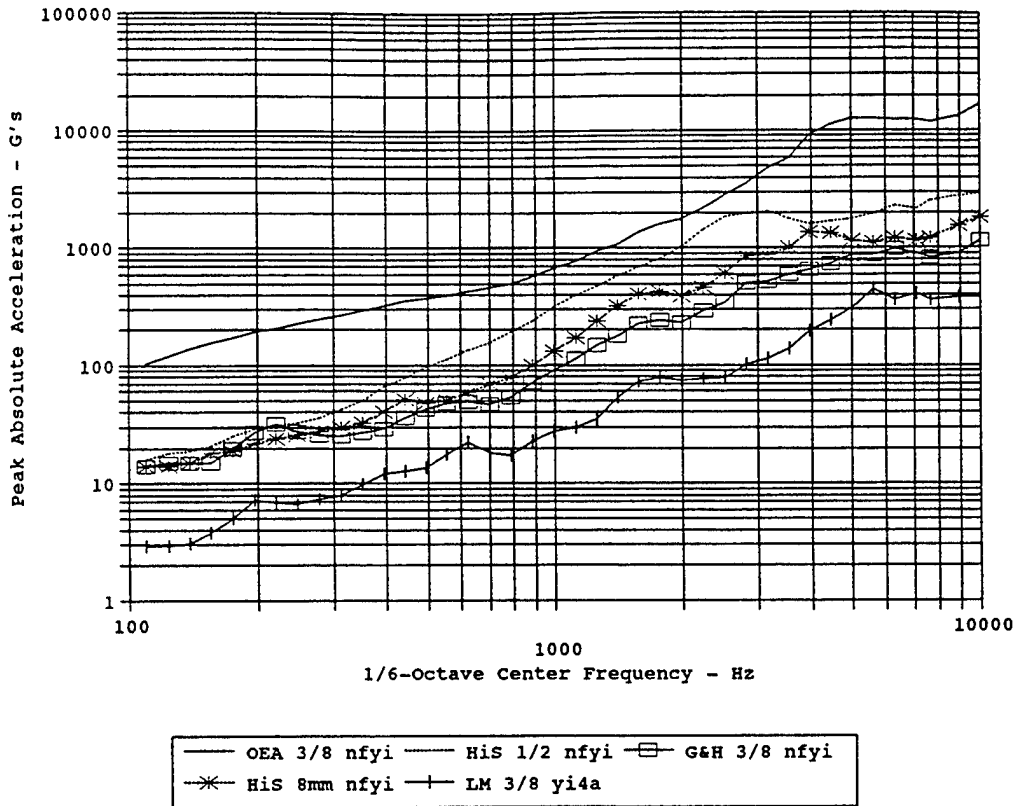


**Figure 10(a). Device Comparison, with Masses, Combined Normal & In-Plane Resultant, SRS (Q=10), 95th Percentile Levels.**

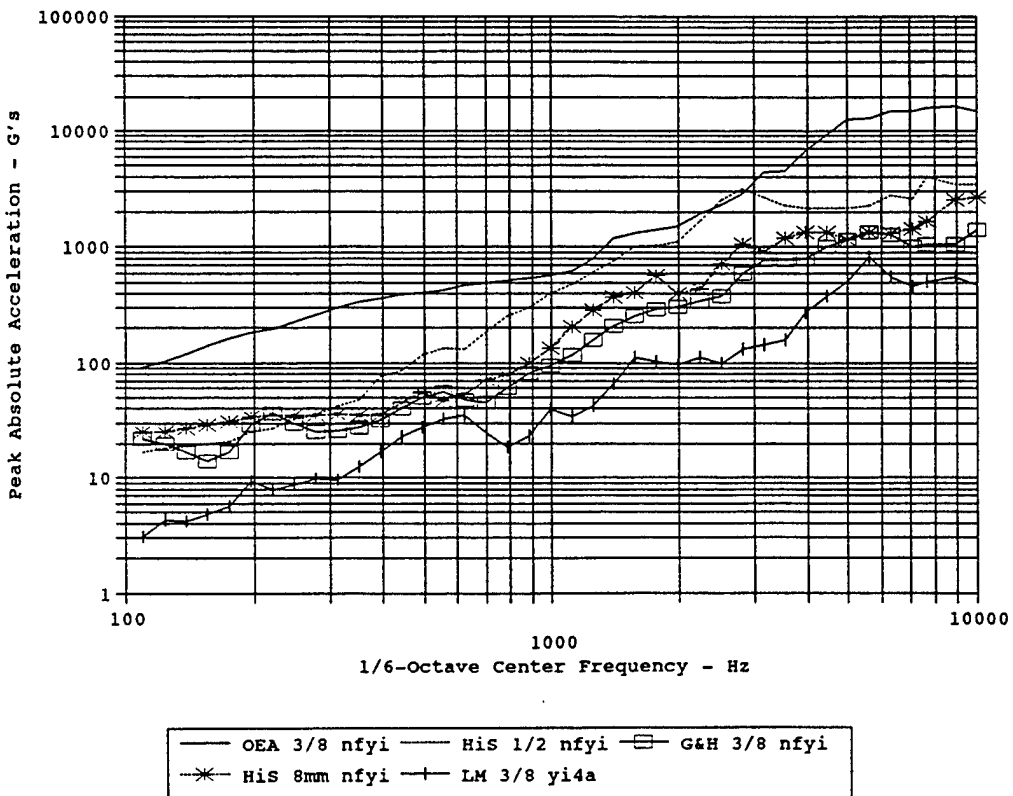


**Figure 10(b). Device Comparison, with Masses, Combined Normal & In-Plane Resultant, SRS (Q=10), Maximum Measured Levels.**

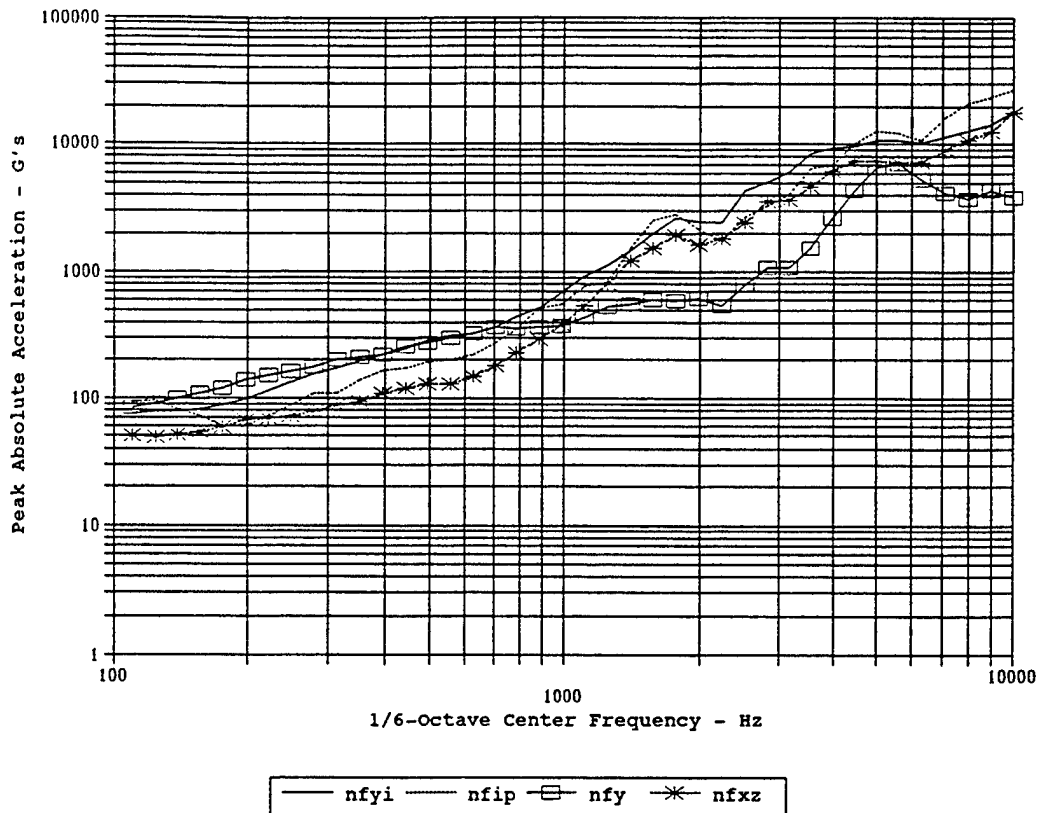


**Figure 11(a). OEA 3/8", Bare Panel, 7000 lb., Various Axis Groupings, SRS (Q=10), 95th Percentile Levels.**

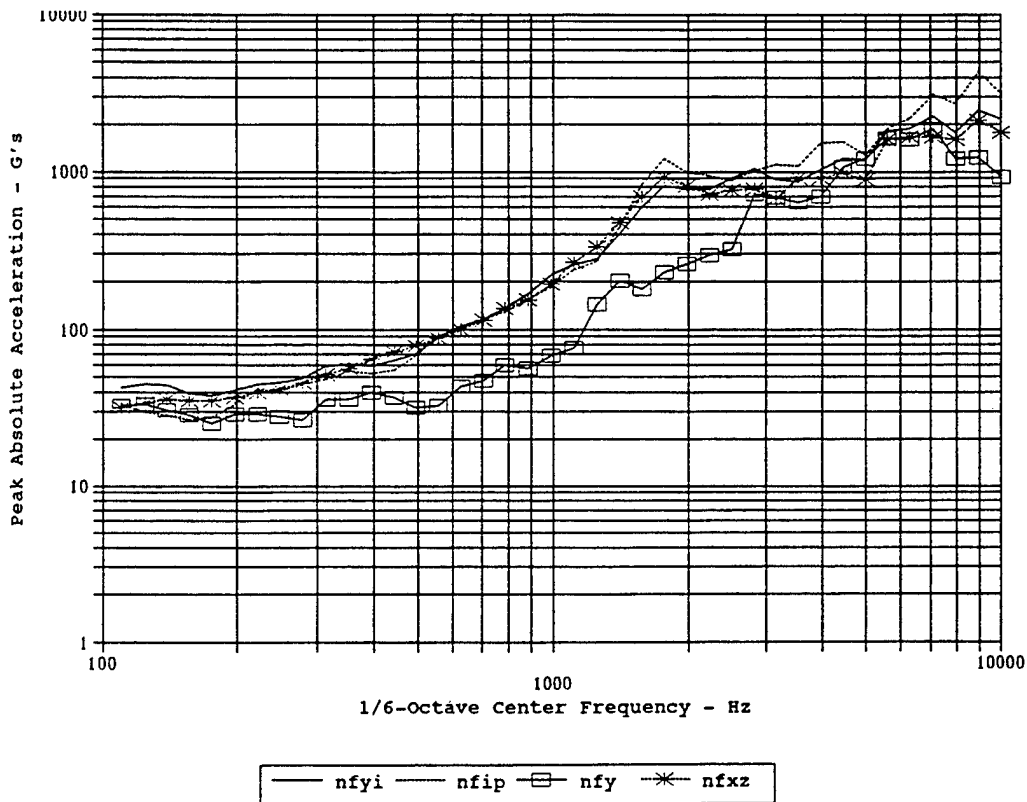
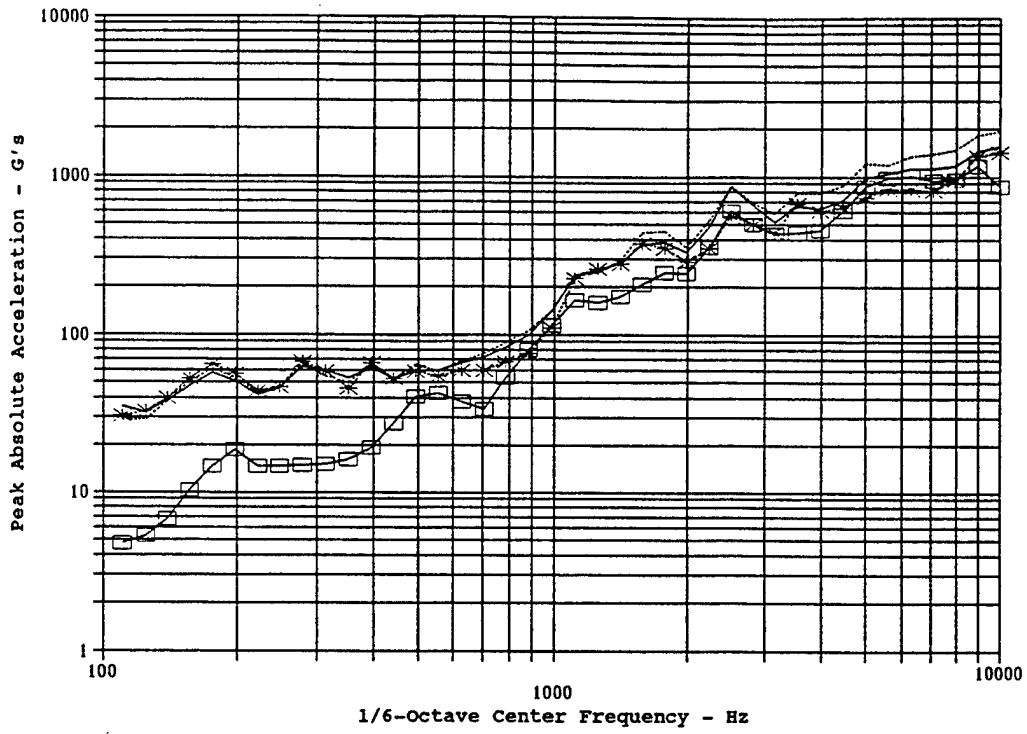


**Figure 11(b). HiS 1/2", Bare Panel, 7000 lb., Various Axis Groupings, SRS (Q=10), 95th Percentile Levels.**



— nfyi — nfip —□— nfy —\*— nfxz

**Figure 11(c). G&H 3/8", Bare Panel, 7000 lb., Various Axis Groupings, SRS (Q=10), 95th Percentile Levels.**

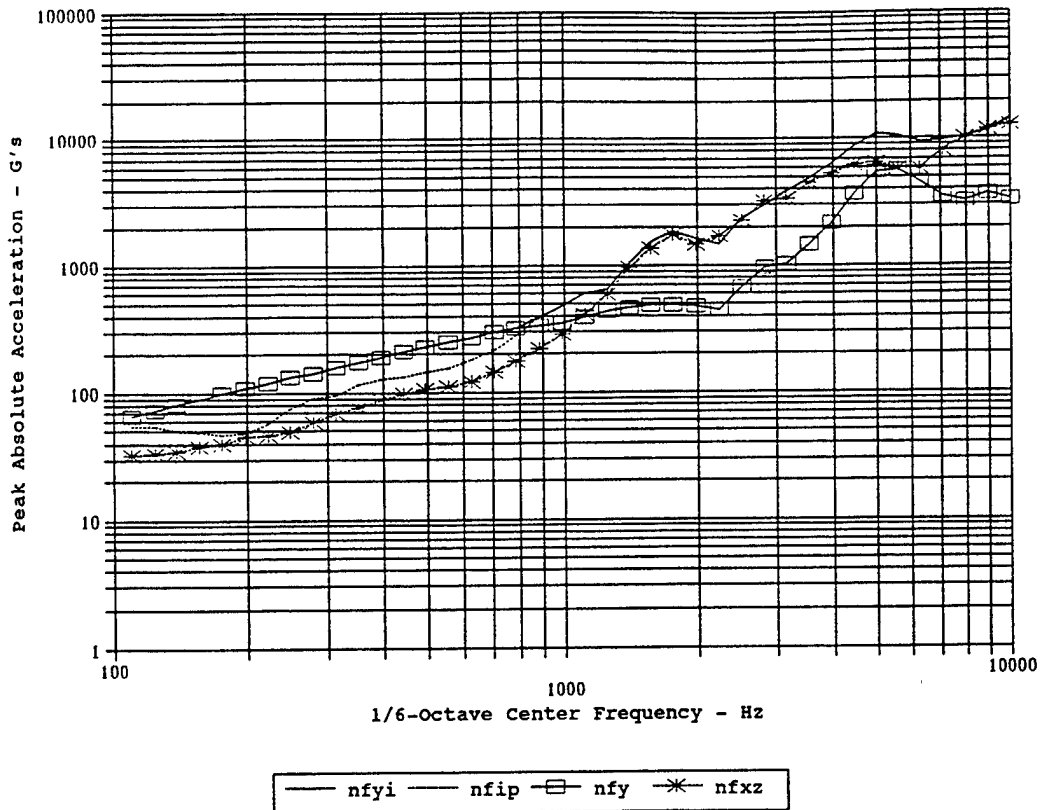


**Figure 12(a). OEA 3/8", Bare Panel, 7000 lb., Various Axis Groupings, SRS (Q=10), Maximum Measured Levels.**

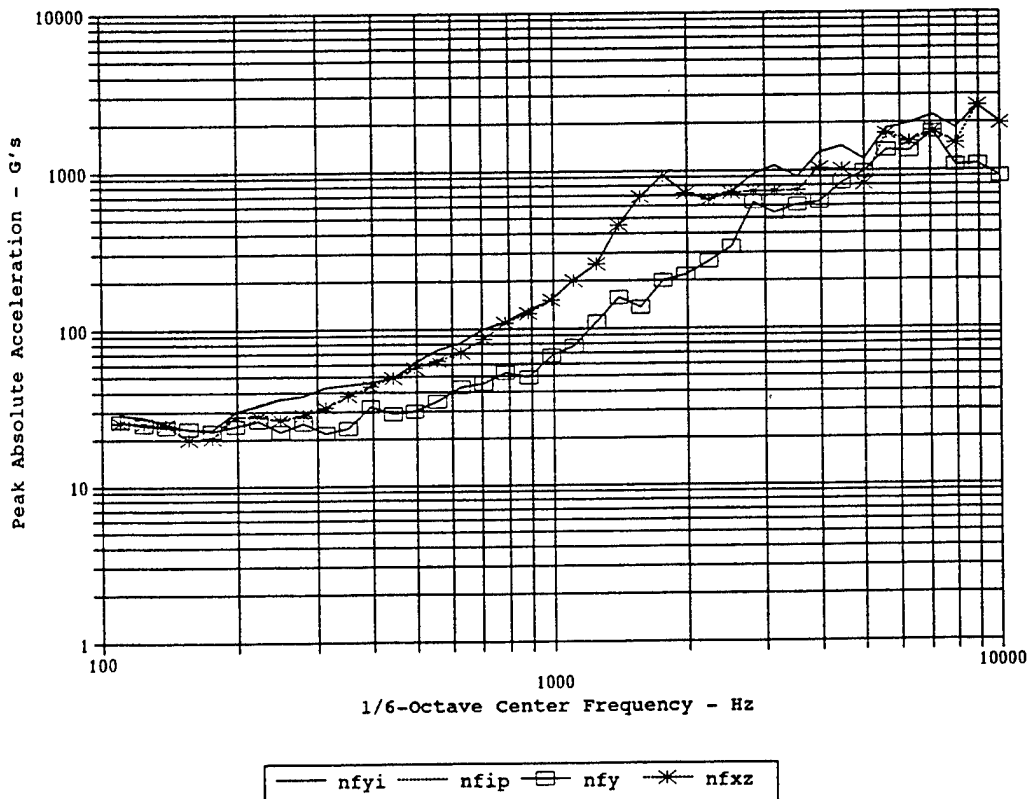
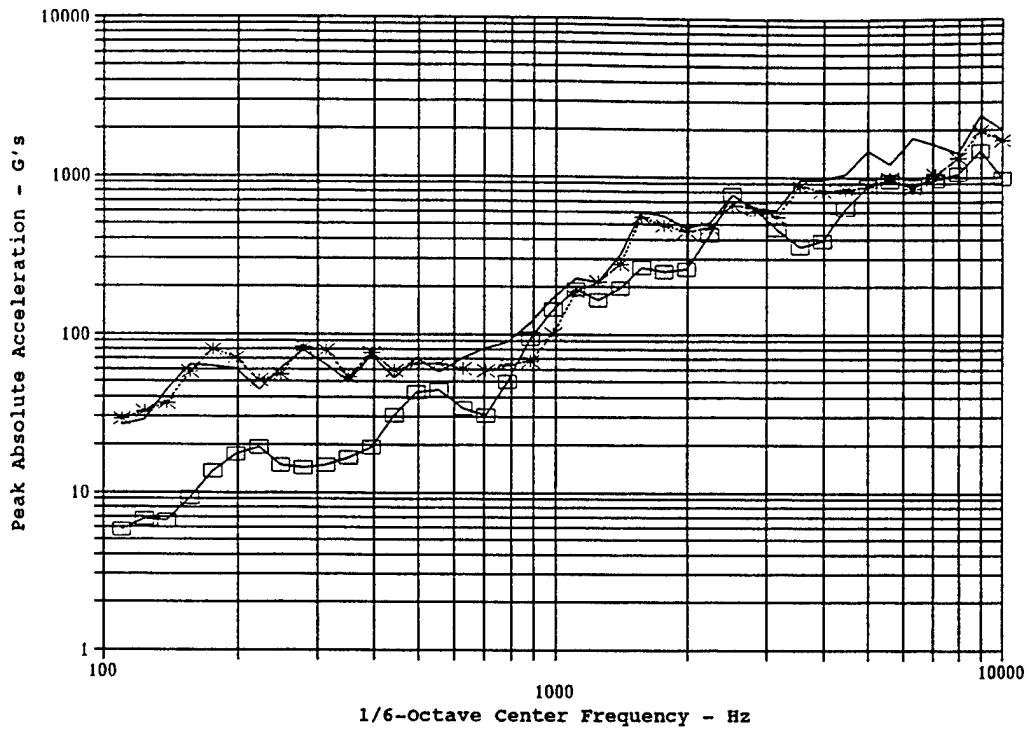


**Figure 12(b). HiS 1/2", Bare Panel, 7000 lb., Various Axis Groupings, SRS (Q=10), Maximum Measured Levels.**



— nfyi — nfip —□— nfy —\*— nfxz

**Figure 12(c). G&H 3/8", Bare Panel, 7000 lb., Various Axis Groupings, SRS (Q=10), Maximum Measured Levels.**

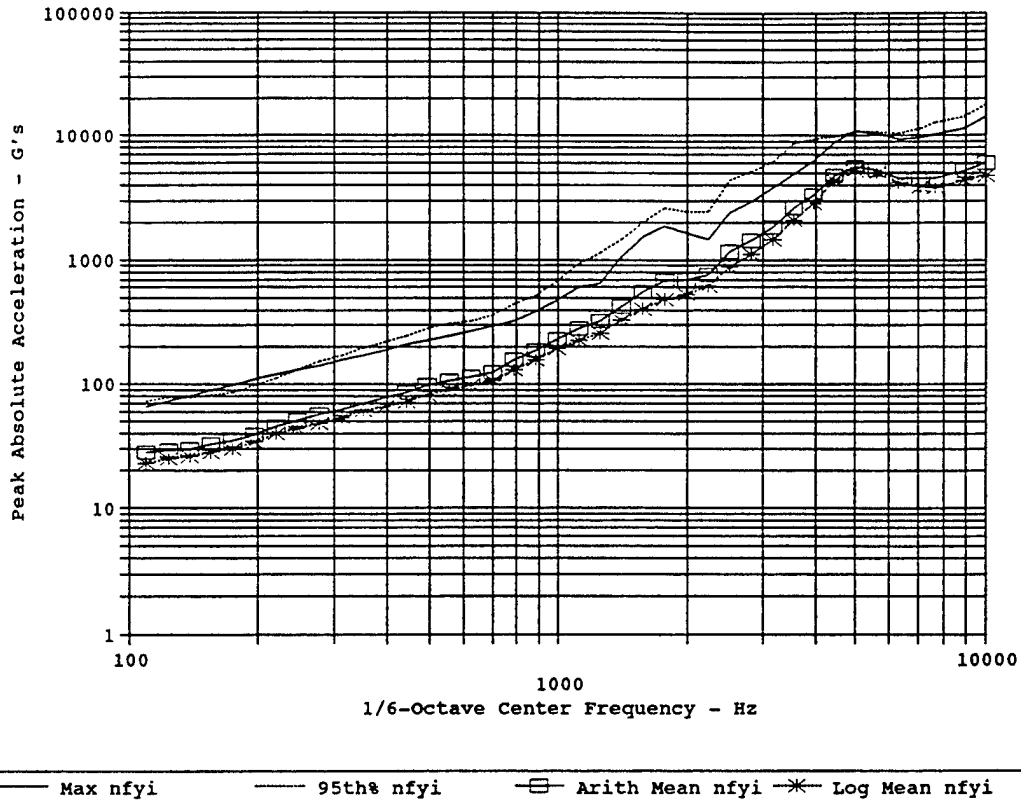


**Figure 13(a). OEA 3/8", Bare Panel, 7000 lb., Combined Normal & In-Plane Resultant, SRS (Q=10), Log-Normal Statistical Features.**

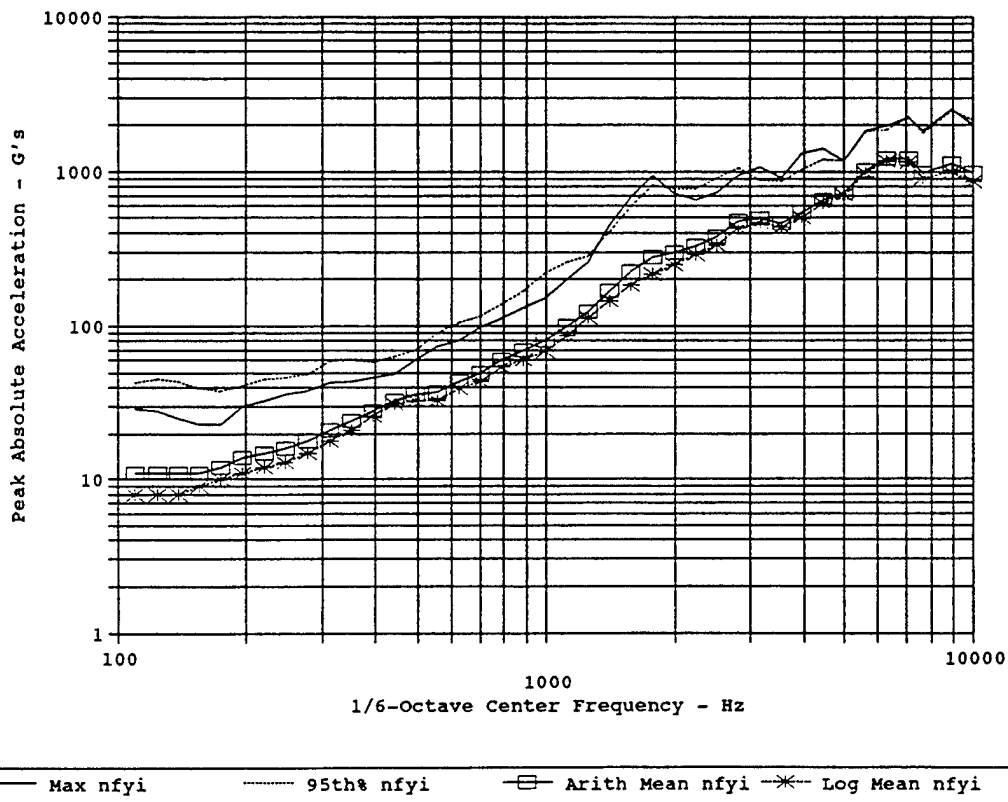


**Figure 13(b). HiS 1/2", Bare Panel, 7000 lb., Combined Normal & In-Plane Resultant, SRS (Q=10), Log-Normal Statistical Features.**

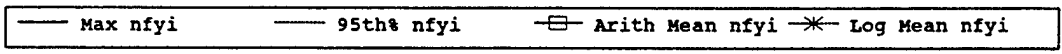
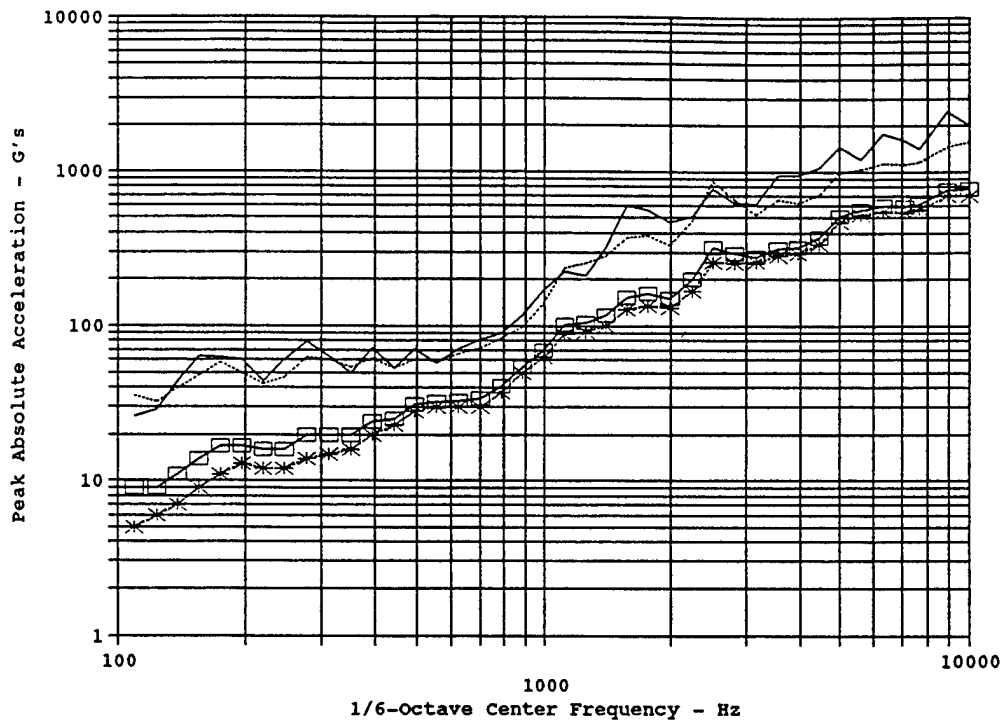


**Figure 13(c). G&H 3/8", Bare Panel, 7000 lb., Combined Normal & In-Plane Resultant, SRS (Q=10), Log-Normal Statistical Features.**

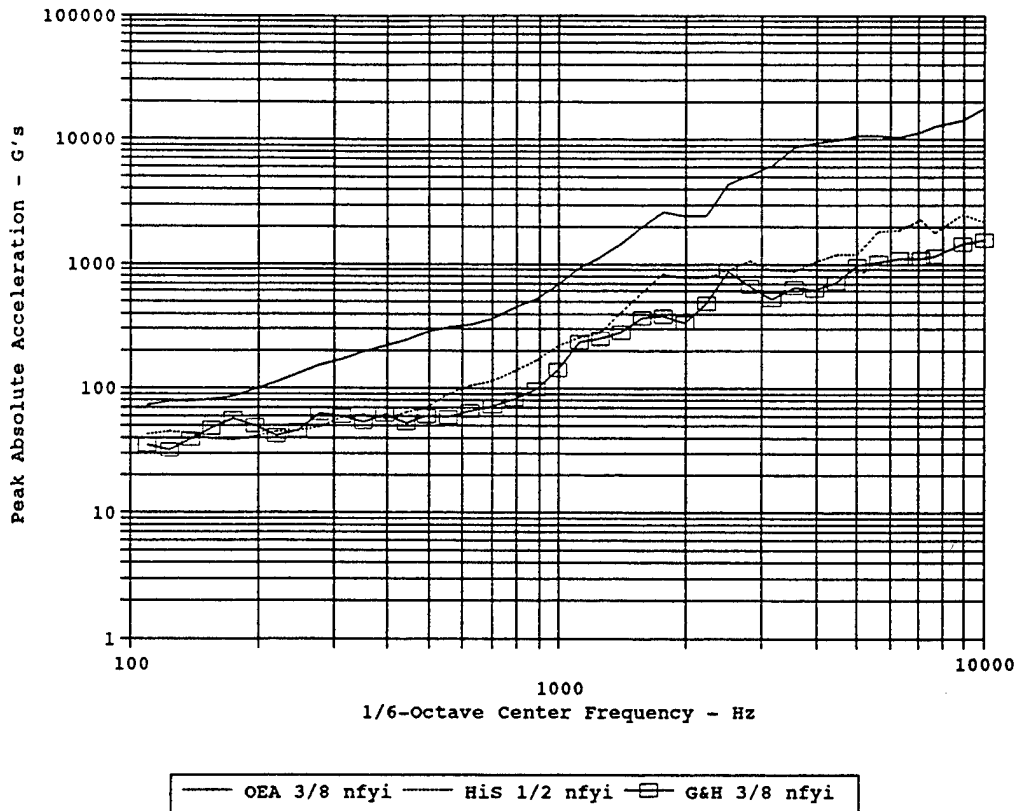


**Figure 14(a). Device Comparison, Bare Panel, 7000 lb., Combined Normal & In-Plane Resultant, SRS (Q=10), 95th Percentile Levels.**

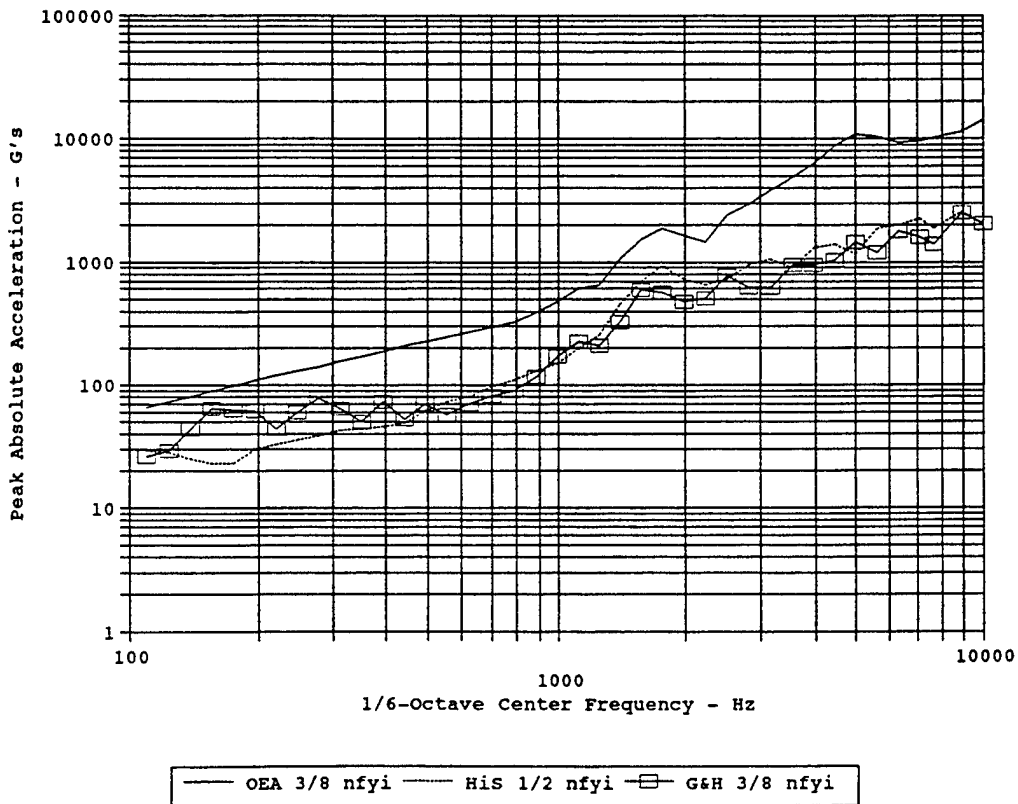


**Figure 14(b). Device Comparison, Bare Panel, 7000 lb., Combined Normal & In-Plane Resultant, SRS (Q=10), Maximum Measured Levels.**

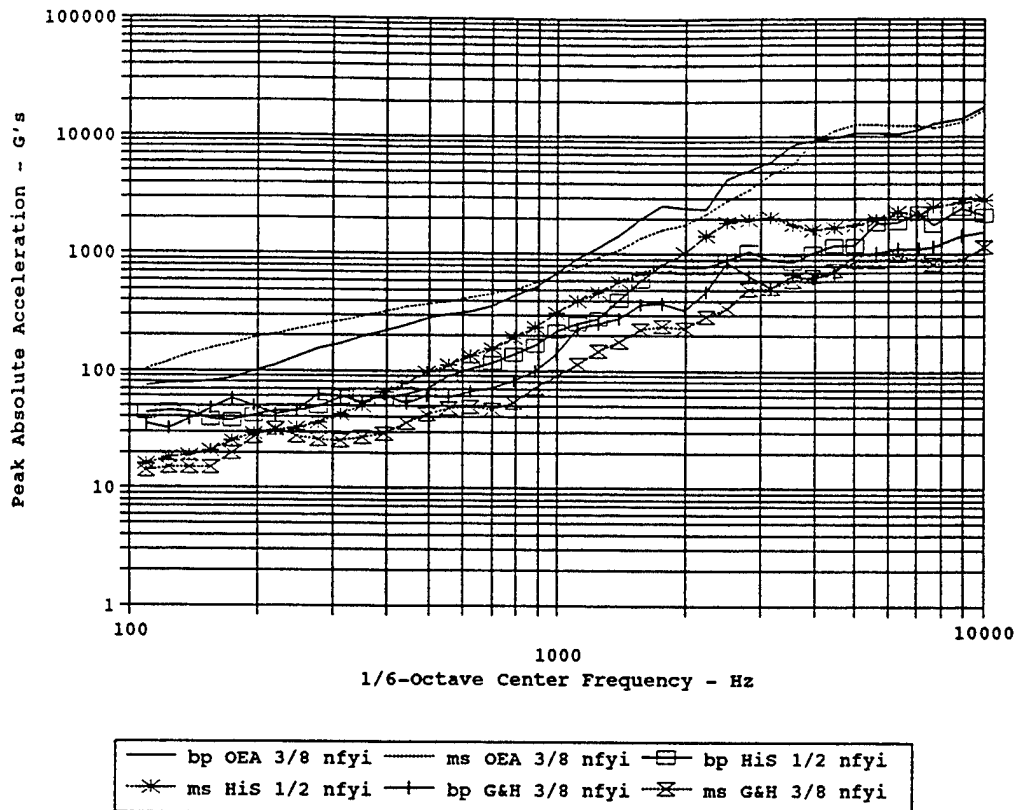


**Figure 15(a). Device Comparison, with & without Masses, 7000 lb., Combined Normal & In-Plane Resultant, SRS (Q=10), 95th Percentile Levels.**

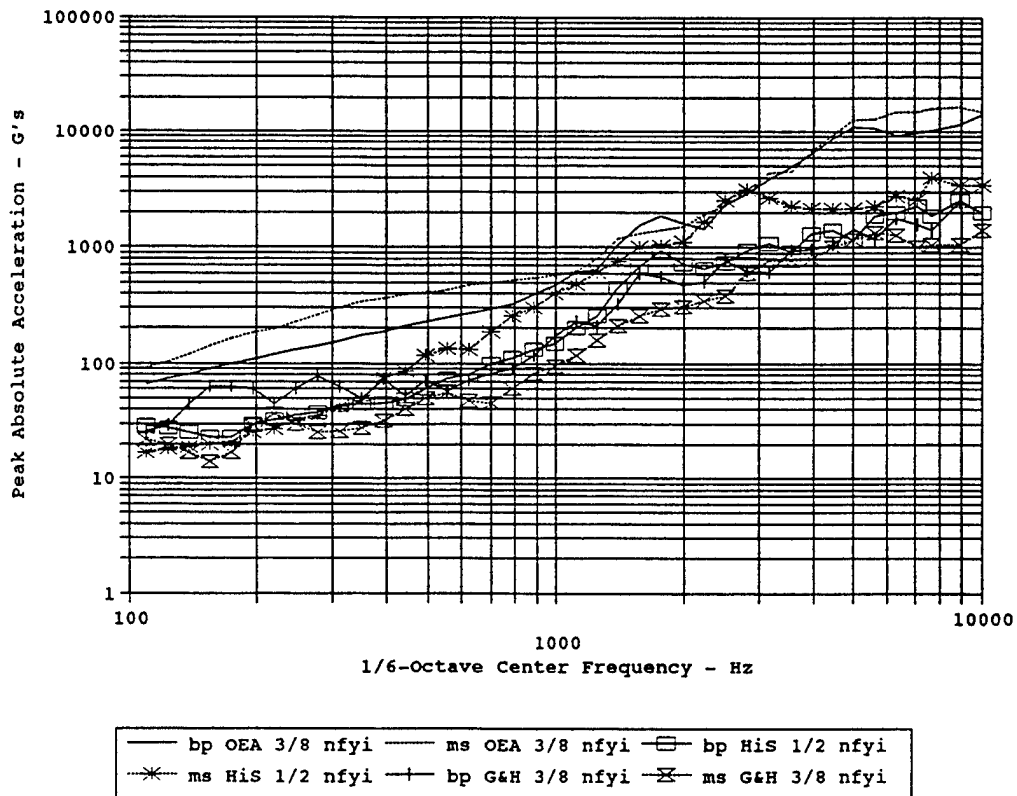


**Figure 15(b). Device Comparison, with & without Masses, 7000 lb., Combined Normal & In-Plane Resultant, SRS (Q=10), Maximum Measured Levels.**

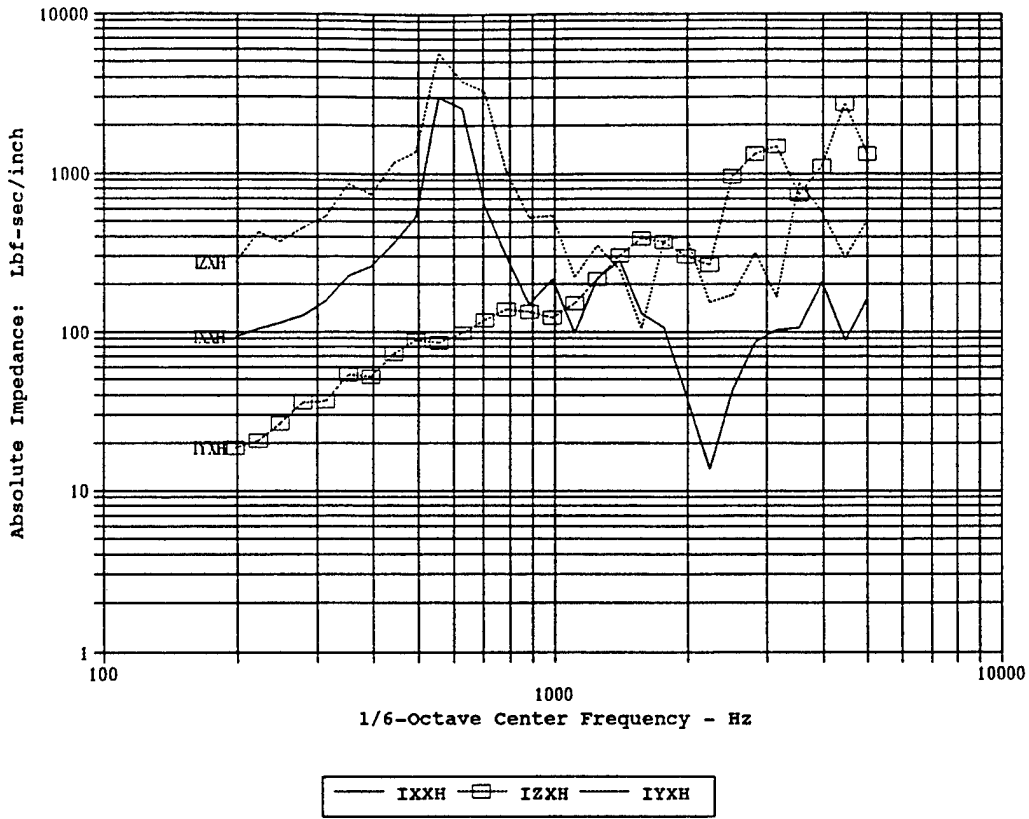


**Figure 16. 3/8" Release Device Mounting Point Impedances, X-Direction Tap.**

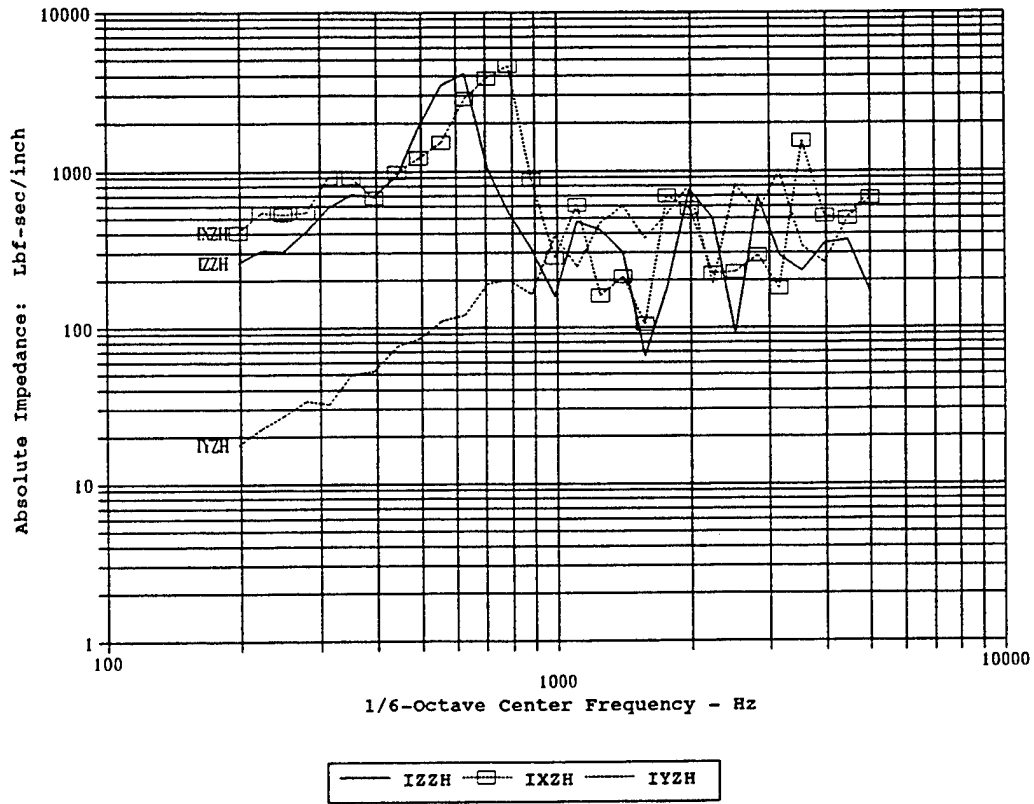
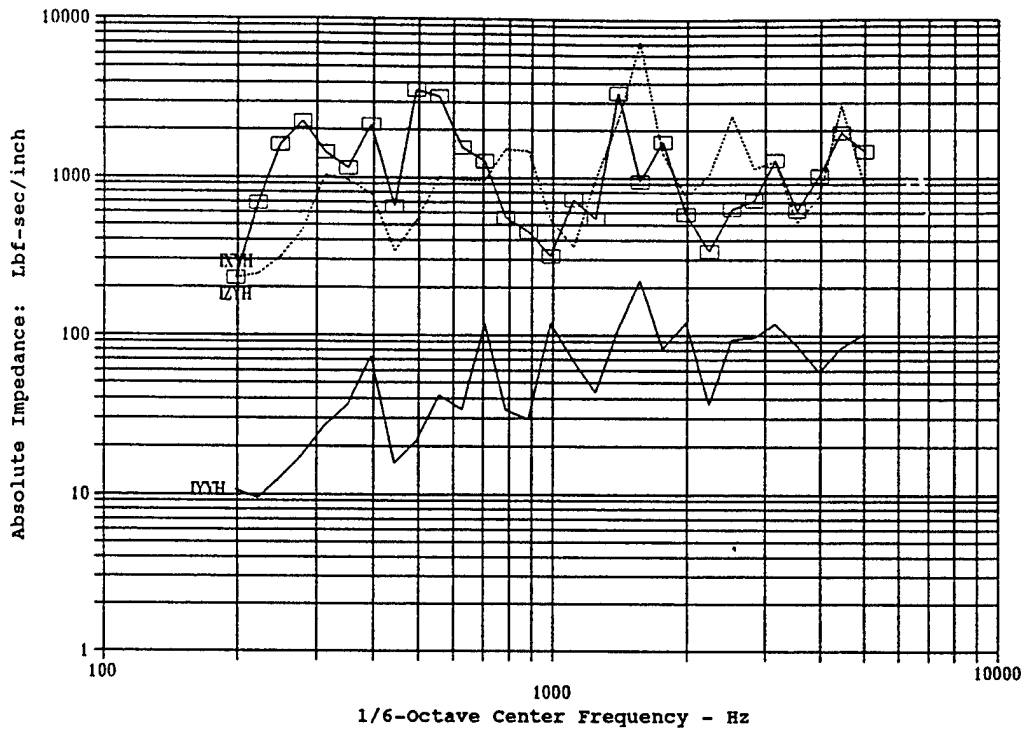


**Figure 17. 3/8" Release Device Mounting Point Impedances, Z-Direction Tap.**



— IYH — IXYH — IZYH

**Figure 18. 3/8" Release Device Mounting Point Impedances, Y-Direction Tap.**

Freq Hz	Arithmetic Mean nfyi	Log Mean nfyi	Standard Deviation	95th Percentile nfyi	Maximum nfyi	95th Percentile nfip	Maximum nfip	95th Percentile nfy	Maximum nfy	95th Percentile nfzx	Maximum nfzx
110	40	34	1.861	103	92	97	92	108	88	81	86
124	46	38	1.915	121	105	113	105	124	95	90	91
139	51	42	1.933	138	121	134	121	135	105	99	97
156	57	46	1.967	156	140	161	140	149	115	109	101
175	62	50	1.987	172	164	184	164	161	128	119	114
197	69	55	2.011	193	184	203	184	173	140	129	124
221	75	60	1.996	208	195	220	195	184	155	135	134
248	82	66	1.996	227	225	245	225	199	172	141	143
278	90	73	1.973	247	260	265	260	209	186	151	148
313	99	80	1.965	268	299	307	299	226	205	166	163
351	109	87	1.992	298	339	355	339	251	226	178	181
394	119	95	1.997	327	365	402	365	279	250	189	189
442	130	104	1.980	354	391	428	391	305	272	202	193
496	141	115	1.940	375	411	418	411	342	295	220	225
557	151	124	1.907	393	430	428	430	351	328	237	220
625	165	137	1.892	427	468	460	468	374	365	252	251
702	184	154	1.851	464	500	492	500	396	395	282	259
787	204	174	1.801	497	522	529	522	409	428	324	298
884	230	196	1.816	571	545	562	545	438	475	389	340
992	264	226	1.833	668	571	591	571	477	513	514	431
1114	304	258	1.850	776	629	720	629	463	533	692	572
1250	363	304	1.871	931	786	956	786	446	542	898	732
1403	451	384	1.778	1075	1198	1253	1198	474	597	1012	921
1575	533	442	1.880	1367	1293	1457	1293	552	643	1123	1004
1768	614	510	1.895	1601	1392	1593	1392	685	688	1286	1164
1984	714	605	1.816	1760	1507	1708	1507	668	715	1479	1403
2227	869	729	1.851	2195	1917	2028	1917	788	733	1763	1669
2500	1101	925	1.870	2836	2292	2496	2292	1278	1472	2252	2331
2806	1423	1205	1.834	3566	2831	3215	2831	1702	2501	2885	3306
3150	1912	1615	1.837	4794	4320	4392	4320	2052	2621	3679	4314
3536	2419	2075	1.781	5830	4454	5404	4454	2319	2464	5046	5283
3969	3429	2845	1.912	9076	6705	7929	6705	3624	3462	6614	6397
4454	4534	3848	1.831	11360	9302	10550	9302	5208	4444	8321	7862
5000	5365	4629	1.750	12601	12659	14386	12659	6598	6330	8822	7779
5612	5670	4944	1.692	12663	13062	14121	13062	6330	7503	8731	7844
6300	5614	4899	1.685	12463	14858	14501	14858	5986	6793	8999	8724
7071	5161	4369	1.780	12253	14822	15646	14822	6148	5742	9316	10744
7637	5148	4385	1.748	11905	16178	15537	16178	6129	7231	9670	12043
8909	5654	4818	1.765	13314	16467	15678	16467	5553	7110	10583	12300
10000	6447	5293	1.900	16680	14781	16034	14781	4665	4530	12471	11813

**Table A-1(a): OEA 3/8", with Masses, 7000 lb., SRS (Q=10), Log-Normal Statistical Features of Combined Normal & In-Plane, & Various Axis Groupings. Number of Samples = 31 Gumbel Factor = 0.9194**

Freq Hz	Arithmetic Mean nfyi	Log Mean nfyi	Standard Deviation	95th Percentile nfyi	Maximum nfyi	95th Percentile nfiy	Maximum nfiy	95th Percentile nfxz	Maximum nfxz
110	6	5	1.946	16	17	23	17	9	14
124	7	5	1.958	18	18	24	18	10	15
139	7	6	1.955	19	19	24	19	10	12
156	8	6	2.016	21	20	26	20	11	12
175	9	7	1.998	25	21	28	21	15	15
197	11	9	1.977	29	25	30	25	21	16
221	12	10	1.866	31	27	33	27	22	12
248	13	11	1.820	33	33	34	33	20	16
278	15	12	1.837	36	35	33	35	23	17
313	17	14	1.833	42	42	38	42	29	23
351	21	18	1.809	50	48	46	45	40	33
394	25	21	1.911	66	76	60	52	57	37
442	30	24	1.981	79	86	77	68	63	44
496	36	29	1.989	96	116	92	79	74	55
557	44	37	1.899	113	135	106	90	94	69
625	54	45	1.858	134	131	132	131	106	93
702	62	52	1.878	156	190	167	190	104	118
787	73	59	1.958	192	253	228	253	104	176
884	89	70	2.016	239	305	321	305	111	235
992	118	94	1.997	315	400	410	400	149	358
1114	152	121	1.986	403	485	548	485	175	526
1250	188	151	1.932	478	608	711	608	213	668
1403	243	202	1.831	585	750	805	750	343	794
1575	274	221	1.919	693	1017	938	1020	306	780
1768	310	246	1.986	818	1026	1010	1030	271	773
1984	385	306	2.009	1040	1109	1160	1110	360	916
2227	521	407	2.048	1429	1667	1560	1670	443	1270
2500	672	512	2.088	1861	2510	2360	2510	572	1740
2806	749	570	2.029	1972	3104	2910	3100	511	2400
3150	795	629	1.952	2032	2682	3120	2680	705	2420
3536	777	658	1.768	1785	2274	2560	2270	976	1900
3969	740	643	1.699	1630	2127	2130	2130	1010	1500
4454	790	696	1.666	1703	2136	2060	2140	1150	1610
5000	923	842	1.526	1767	2164	2070	2160	1570	1440
5612	1076	1002	1.470	1969	2265	2290	2270	1800	1790
6300	1271	1186	1.459	2300	2778	2870	2780	1810	1810
7071	1211	1129	1.439	2129	2607	2790	2610	1520	1760
7637	1325	1187	1.547	2552	3992	3820	3990	1390	1950
8909	1365	1213	1.602	2773	3433	3840	3430	1370	2760
10000	1277	1094	1.739	2888	3469	3480	3470	1070	3450

**Table A-1(b): HiS 1/2", with Masses, 7000 lb., SRS (Q=10), Log-Normal Statistical Features of Combined Normal & In-Plane, & Various Axis Groupings. Number of Samples = 45 Gumbel Factor = 0.9381**

Freq Hz	Arithmetic Mean nfyj	Log Mean nfyi	Standard Deviation	95th Percentile nfyj	Maximum nfyj	95th Percentile nfip	Maximum nfip	95th Percentile nfy	Maximum nfy	95th Percentile nfzx	Maximum nfzx
110	5	4	2.042	14	22	15	14	14	22	11	14
124	6	4	2.013	15	20	16	20	15	19	11	20
139	6	4	2.002	15	17	16	17	14	17	11	17
156	6	5	1.853	15	14	14	13	15	14	10	13
175	8	7	1.882	20	17	15	16	25	17	11	16
197	10	9	1.907	27	29	15	14	41	29	12	14
221	12	10	1.995	32	37	16	15	53	37	13	15
248	10	9	1.972	28	30	21	19	38	30	12	17
278	10	8	1.926	26	25	22	23	30	25	12	18
313	10	9	1.867	25	26	25	26	26	21	12	18
351	11	10	1.794	27	28	28	28	25	24	13	18
394	13	11	4.757	29	32	31	29	27	32	15	16
442	15	13	1.793	36	40	37	36	33	40	21	22
496	19	16	1.703	42	50	43	39	40	50	26	26
557	23	21	1.619	48	56	49	46	50	56	33	30
625	24	21	1.601	49	48	50	47	48	48	33	32
702	24	22	1.542	47	46	54	46	38	38	39	43
787	27	25	1.563	54	61	66	61	41	35	48	58
884	35	31	1.597	71	83	89	83	57	50	64	74
992	44	40	1.591	90	95	110	95	75	67	93	95
1114	56	51	1.595	115	118	129	118	101	89	144	118
1250	70	63	1.639	149	161	167	161	138	103	170	161
1403	80	69	1.722	179	210	214	210	155	141	190	170
1575	97	81	1.802	229	258	285	258	142	174	255	249
1768	112	98	1.689	245	294	337	294	148	147	268	281
1984	120	110	1.520	230	306	301	306	158	133	238	284
2227	154	141	1.526	296	351	365	351	194	196	314	351
2500	185	170	1.512	351	379	419	379	264	283	338	379
2806	244	216	1.636	511	602	666	602	321	318	462	440
3150	258	231	1.582	517	776	686	776	287	306	442	457
3536	297	266	1.583	596	774	747	774	309	314	523	532
3969	348	320	1.514	662	798	783	798	524	496	560	623
4454	414	386	1.441	732	998	921	998	572	769	688	880
5000	513	482	1.410	880	1155	1151	1155	665	782	825	1092
5612	509	477	1.416	878	1327	1047	1327	784	782	753	1046
6300	568	533	1.415	981	1274	1074	1274	962	1076	757	1103
7071	515	484	1.427	904	1006	984	1006	892	975	767	817
7637	488	461	1.401	833	1061	1026	1061	699	718	737	838
8909	510	478	1.432	898	1068	1007	1068	718	710	792	835
10000	564	500	1.623	1168	1407	1407	1407	555	649	918	1198

**Table A-1(c): G&H 3/8", with Masses, 7000 lb., SRS (Q=10), Log-Normal Statistical Features of Combined Normal & In-Plane, & Various Axis Groupings. Number of Samples = 45 Gumbel Factor = 0.9381**

Freq Hz	Arithmetic Mean nfyi	Log Mean nfyi	Standard Deviation	95th Percentile nfyi	Maximum nfyi	95th Percentile nfip	Maximum nfip	95th Percentile nfy	Maximum nfy	95th Percentile nfzx	Maximum nfzx
110	5	4	2.152	14	25	11	14	15	25	10	26
124	5	4	2.097	14	25	12	13	15	25	10	26
139	5	4	2.097	15	27	12	14	15	27	10	27
156	6	4	2.234	18	29	14	17	17	29	10	29
175	7	5	2.165	19	31	16	17	18	31	11	30
197	8	6	2.121	22	34	18	16	21	34	12	32
221	8	6	2.171	24	35	20	17	20	35	13	34
248	9	7	2.146	26	35	22	17	19	35	14	34
278	9	7	2.127	28	35	22	18	20	35	15	35
313	11	9	2.053	30	36	24	22	23	36	16	35
351	12	10	1.977	33	35	26	26	25	35	18	36
394	14	12	2.027	40	35	30	27	40	35	22	36
442	18	14	2.070	51	46	35	39	57	46	26	36
496	19	16	1.890	48	55	36	35	49	55	28	35
557	21	19	1.756	50	47	41	42	52	47	32	34
625	25	22	1.753	59	54	48	49	59	54	40	37
702	29	25	1.767	69	71	60	61	63	71	51	44
787	35	31	1.709	78	79	77	79	62	67	68	57
884	43	37	1.760	100	99	111	99	67	60	94	74
992	56	49	1.758	131	136	144	136	84	105	139	110
1114	70	60	1.812	170	209	189	209	105	118	218	201
1250	92	75	1.918	237	286	301	286	140	107	300	318
1403	127	104	1.896	321	373	434	373	212	170	362	358
1575	157	127	1.961	415	409	506	409	281	230	432	390
1768	175	144	1.861	428	571	531	571	274	234	452	475
1984	173	152	1.701	387	402	421	402	266	228	376	345
2227	204	177	1.727	463	442	532	442	283	266	401	416
2500	266	229	1.744	608	720	775	720	339	308	510	483
2806	344	281	1.877	850	1053	1216	1053	408	365	707	798
3150	376	321	1.758	864	917	1122	917	406	367	791	758
3536	476	423	1.630	998	1202	1130	1202	517	545	915	889
3969	604	531	1.706	1358	1328	1343	1328	781	756	1056	1002
4454	662	603	1.567	1327	1324	1440	1324	882	829	1143	1331
5000	616	570	1.491	1151	1156	1284	1156	1063	1110	926	1077
5612	608	563	1.478	1118	1322	1290	1322	1036	1057	862	908
6300	664	616	1.465	1206	1302	1409	1291	1072	1302	837	1016
7071	655	611	1.434	1152	1436	1321	1436	1070	1432	807	997
7637	659	609	1.478	1210	1653	1408	1653	1118	1327	984	1374
8909	698	601	1.710	1544	2520	2032	2520	1229	1318	1290	1956
10000	763	634	1.816	1809	2649	2527	2649	930	967	1628	2157

**Table A-1(d): HiS 8 mm, with Masses, 2700 lb., SRS (Q=10), Log-Normal Statistical Features of Combined Normal & In-Plane, & Various Axis Groupings. Number of Samples = 43 Gumbel Factor = 0.9360**

Freq Hz	Arithmetic Mean y <sub>i4a</sub>	Log Mean y <sub>i4a</sub>	Standard Deviation	95th Percentile y <sub>i4a</sub>	Maximum y <sub>i4a</sub>	95th Percentile ip <sub>4a</sub>	Maximum ip <sub>4a</sub>	95th Percentile y <sub>4a</sub>	Maximum y <sub>4a</sub>	95th Percentile xz <sub>4a</sub>	Maximum xz <sub>4a</sub>
110	1.4	1.3	1.580	2.9	3.1	3	3	3	3	2	2
124	1.4	1.3	1.589	2.9	4.3	3	4	2	2	2	2
139	1.5	1.3	1.642	3.1	4.2	4	4	2	2	2	2
156	1.7	1.5	1.697	3.8	4.8	4	5	3	3	2	2
175	2.1	1.8	1.802	5.1	5.7	5	6	5	5	2	2
197	2.9	2.4	1.880	7.2	9.3	5	7	10	9	2	2
221	2.9	2.5	1.807	6.9	7.9	5	8	9	8	2	2
248	2.8	2.4	1.795	6.7	8.8	7	9	7	6	2	2
278	3	2.5	1.826	7.3	9.7	7	10	8	8	2	3
313	3.4	2.9	1.791	8	9.6	7	9	8	10	3	5
351	4.4	3.9	1.679	9.7	12.3	9	9	11	12	4	8
394	5.3	4.5	1.755	12.2	16.8	10	11	15	17	6	11
442	5.4	4.5	1.819	12.8	23	10	10	15	23	6	9
496	6	5.1	1.745	13.6	27.6	11	12	17	28	7	10
557	7.9	6.7	1.741	17.8	32.6	12	15	23	33	13	13
625	9.6	8.1	1.772	22.2	35	15	18	29	35	15	14
702	9	8.1	1.584	18.1	24.7	13	12	23	25	11	12
787	9.4	8.7	1.469	17.1	18.7	16	17	19	19	11	13
884	12	11.1	1.523	23.1	23.4	21	19	25	23	15	16
992	13.3	11.8	1.632	27.8	39.7	29	35	29	40	26	33
1114	14	12.4	1.647	29.6	33.9	38	34	24	33	38	34
1250	16.8	14.9	1.638	35.5	42.4	45	42	28	35	40	40
1403	23.1	19.6	1.783	54.1	67	70	67	39	44	51	67
1575	30.4	24.8	1.850	72.9	110.7	113	111	36	38	70	99
1768	33.4	28.3	1.777	77.5	103.8	105	104	45	44	72	83
1984	36.5	32.3	1.621	75.3	98.1	99	98	50	62	71	98
2227	39.9	36.1	1.533	76.4	111.9	106	112	44	43	89	112
2500	43.8	40.7	1.455	78.6	98.8	105	99	46	44	87	99
2806	53.3	48.3	1.537	102.6	131.6	139	132	56	57	112	132
3150	59.4	54	1.524	113.1	143.6	150	144	54	56	106	110
3536	77	71.8	1.455	138.5	158.3	159	158	85	80	124	117
3969	102.6	93.9	1.523	196.5	277.5	212	278	144	187	167	235
4454	135.5	125.7	1.460	244.1	385.9	307	386	189	202	218	326
5000	176.8	165.2	1.424	307.1	504.6	376	505	264	257	266	404
5612	212.5	183.8	1.664	448.8	835.6	574	836	386	482	405	635
6300	201.4	187	1.453	360.2	552.9	435	553	297	328	362	453
7071	221.7	204	1.496	413.7	458.8	469	458	383	459	396	458
7637	201.6	185.9	1.477	368.2	508.5	505	508	255	268	384	428
8909	203.4	185.6	1.512	383.2	558.4	529	558	226	235	375	529
10000	179.1	157.2	1.652	378.9	467.6	472	468	169	174	313	372

**Table A-1(e): LM 3/8", with Masses, Combined 4000 & 4200 lb., SRS (Q=10), Log-Normal Statistical Features of Combined Normal & In-Plane, & Various Axis Groupings. Number of Samples = 45 Gumbel Factor = 0.9381**

Freq Hz	Arithmetic Mean yi42	Log Mean yi42	Standard Deviation	95th Percentile yi42	Maximum yi42
110	1.6	1.5	1.592	3.6	3.1
124	1.6	1.5	1.586	3.5	4.3
139	1.6	1.5	1.527	3.3	4.2
156	1.8	1.7	1.369	3.2	2.8
175	2.1	2	1.441	4	4.2
197	2.8	2.6	1.557	6	5.6
221	3.1	2.9	1.484	6	6.5
248	3.2	2.9	1.500	6.3	6.5
278	3.4	3.1	1.583	7.4	8
313	4.4	4	1.576	9.5	9.6
351	6	5.3	1.644	13.7	12.3
394	7.6	6.6	1.748	19	16.8
442	7.7	6.5	1.767	19.2	23
496	8.5	7.3	1.680	19.6	27.6
557	11	9.5	1.689	25.6	32.6
625	12.9	10.9	1.736	31	35
702	10	8.9	1.610	21.8	24.7
787	9.1	8.2	1.562	19	18.7
884	11.3	10.1	1.633	25.6	23.4
992	15.3	13.3	1.728	37.5	39.7
1114	15.4	13.9	1.587	33.3	32.9
1250	17.9	16.3	1.548	37.2	34.8
1403	25	22.9	1.525	51	45.7
1575	27.4	25.1	1.545	57.2	52.2
1768	31.5	28.7	1.577	68	54
1984	30.7	28.9	1.438	57.5	57.2
2227	31.1	29.7	1.352	52.6	60.2
2500	42.7	40.3	1.409	77.2	79.3
2806	50.8	48.2	1.383	89	101.8
3150	52.5	49.3	1.432	97.4	89.3
3536	75.5	70.6	1.468	145.9	140.3
3969	93.3	85.4	1.565	199.4	160.6
4454	118.8	111.1	1.458	227	220.3
5000	141.9	136.5	1.326	232.8	253.9
5612	130.4	123.9	1.358	221	271.6
6300	157.1	152	1.301	250	250.5
7071	172.8	166.6	1.322	282.5	278.1
7637	167.4	159.7	1.358	285	290.9
8909	180.3	166.4	1.480	349.4	410.3
10000	162.3	138.6	1.739	395	467.6

**Table A-1(f): LM 3/8", with Masses, 4200 lb., SRS (Q=10),  
Log-Normal Statistical Features of Combined Normal & In-Plane, & Various Axis  
Groupings. Number of Samples = 15 Gumbel Factor = 0.8688**

Freq Hz	Arithmetic Mean yi40	Log Mean yi40	Standard Deviation	95th Percentile yi40	Maximum yi40
110	1.3	1.2	1.555	2.6	2.6
124	1.3	1.2	1.570	2.6	3.3
139	1.4	1.2	1.686	3.1	3.7
156	1.7	1.4	1.823	4.1	4.8
175	2.1	1.7	1.959	5.7	5.7
197	2.9	2.3	2.034	8.1	9.3
221	2.8	2.3	1.939	7.5	7.9
248	2.6	2.2	1.896	6.8	8.8
278	2.8	2.3	1.909	7.3	9.7
313	2.9	2.5	1.781	6.9	9.2
351	3.7	3.3	1.586	7.6	8.7
394	4.2	3.8	1.601	8.8	9
442	4.2	3.7	1.694	9.6	8.8
496	4.8	4.3	1.635	10.3	10.5
557	6.3	5.7	1.638	13.8	13.3
625	8	7	1.701	18.2	18.3
702	8.5	7.8	1.573	17.5	15.7
787	9.6	9	1.425	17	14.8
884	12.3	11.6	1.466	23	19.6
992	12.2	11.1	1.577	25.1	35
1114	13.3	11.6	1.672	29.3	33.9
1250	16.3	14.3	1.684	36.4	42.4
1403	22.1	18.2	1.886	56.7	67
1575	31.9	24.7	2.003	85.7	110.7
1768	34.3	28	1.884	87.3	103.8
1984	39.3	34.2	1.698	88.3	98.1
2227	44.3	39.8	1.570	89.4	111.9
2500	44.4	40.9	1.486	83.3	98.8
2806	54.6	48.3	1.615	114.1	131.6
3150	62.9	56.5	1.566	126.2	143.6
3536	77.7	72.4	1.457	142.2	158.3
3969	107.3	98.5	1.501	204	277.5
4454	143.9	133.7	1.448	259.5	385.9
5000	194.3	181.8	1.420	340.8	504.6
5612	253.5	224	1.610	526.1	835.6
6300	223.5	207.4	1.464	410.9	552.9
7071	246.2	225.8	1.523	480.1	458.8
7637	218.6	200.6	1.505	417.6	508.5
8909	215	196.1	1.521	415.8	558.4
10000	187.5	167.4	1.602	389.5	455.4

**Table A-1(g): LM 3/8", with Masses, 4000 lb., SRS (Q=10), Log-Normal Statistical Features of Combined Normal & In-Plane, & Various Axis Groupings. Number of Samples = 30 Gumbel Factor = 0.9175**

Freq Hz	Arithmetic Mean yi35	Log Mean yi35	Standard Deviation	95th Percentile yi35	Maximum yi35
110	1.3	1.2	1.654	3.4	2.1
124	1.2	1.1	1.465	2.4	1.7
139	1.1	1	1.438	2.2	1.9
156	1.3	1.2	1.400	2.4	2
175	1.5	1.4	1.418	2.9	2.1
197	2.4	2.1	1.618	5.7	4.2
221	2.8	2.5	1.667	7.1	5.1
248	2.3	2.1	1.590	5.3	4.5
278	2.6	2.4	1.516	5.6	5.3
313	3.1	2.9	1.498	6.6	6
351	4.3	4	1.522	9.4	8.2
394	5.6	5	1.608	13.3	11.2
442	5.7	4.8	1.841	16.6	14.8
496	7	5.9	1.817	19.8	20.3
557	8.6	7.2	1.775	23.3	23.7
625	6.8	6.2	1.572	15.5	15.7
702	7.2	6.7	1.480	14.9	13.4
787	10.7	10.4	1.288	17.4	15.6
884	16.5	15.7	1.421	32.1	23.1
992	21.1	11.4	1.486	25.5	18.6
1114	11.4	10.5	1.509	24.4	21.4
1250	16.7	15.2	1.594	39.4	25.8
1403	17.9	16	1.701	47.3	29.9
1575	21.1	19	1.631	51.4	42.9
1768	22.5	21.5	1.384	41.8	32.5
1984	24.3	22.8	1.464	49.7	40.6
2227	24.2	23.6	1.287	39.5	34
2500	28.1	27.4	1.266	44.4	37.2
2806	37.6	36.9	1.230	56.2	55.6
3150	43.8	42	1.355	77.9	76.3
3536	63.7	60.2	1.415	122	118.1
3969	107.5	102.7	1.39	200.9	163.1
4454	150.5	145.1	1.349	266.9	187.6
5000	192.4	190	1.183	267.5	248
5612	206.4	199.7	1.313	347.5	323
6300	230.7	222.5	1.333	399.8	338.7
7071	259.6	242.6	1.467	529.8	485.3
7637	167.7	162.1	1.323	286.8	250.8
8909	153.9	150.9	1.235	232.2	218.3
10000	131.6	128.8	1.247	202	192.8

**Table A-1(h): LM 3/8", with Masses, 3500 lb., SRS (Q=10), Log-Normal Statistical Features of Combined Normal & In-Plane, & Various Axis Groupings. Number of Samples = 15 Gumbel Factor = 0.8688**

Freq Hz	Arithmetic Mean yi30	Log Mean yi30	Standard Deviation	95th Percentile yi30	Maximum yi30
110	1.2	1.1	1.610	2.6	2.6
124	1.2	1.1	1.565	2.4	2.6
139	1.2	1.1	1.661	2.6	2.6
156	1.3	1.2	1.676	2.9	3.1
175	1.6	1.5	1.648	3.5	3.8
197	2.1	1.9	1.695	4.7	5.3
221	2.3	2	1.712	5.2	6.2
248	2.4	2.1	1.775	5.7	5.3
278	2.5	2.1	1.802	6	6
313	2.9	2.5	1.758	6.7	8
351	3.6	3.2	1.631	7.6	7.9
394	4.4	3.8	1.696	9.6	11.8
442	4.5	3.9	1.764	10.4	14.9
496	5.2	4.5	1.770	12.2	20.1
557	6.7	5.8	1.720	15	21.3
625	7.1	6.4	1.651	15.3	14.4
702	7.6	6.9	1.549	14.9	16.9
787	9	8.4	1.465	16.5	16.5
884	12.3	11.4	1.485	22.9	21.9
992	12.7	11.6	1.566	25.4	22.8
1114	13.6	11.9	1.680	29.6	35
1250	17.4	15.2	1.706	38.8	41.1
1403	19.5	16.9	1.705	43.1	51.7
1575	27.8	22.6	1.866	67.4	92.5
1768	30.7	26.2	1.747	69.7	79.6
1984	38.4	34.4	1.623	80.5	87.2
2227	38.3	34.1	1.621	79.5	94.7
2500	42.2	37.9	1.586	85	109.4
2806	55.7	49.1	1.649	118	160.5
3150	74.8	66	1.648	158.5	181.2
3536	100.5	90.7	1.573	200.6	241.8
3969	133.8	119.1	1.623	278.3	359.5
4454	140.3	130.7	1.45	250.7	325.5
5000	207.8	188.5	1.545	404.5	482.9
5612	224	200.4	1.581	447.6	616.3
6300	216.8	198.8	1.514	411.7	505
7071	257.3	229.8	1.608	528.6	637.8
7637	183.8	169.5	1.497	344	386.4
8909	193.4	178	1.489	357.7	473
10000	185.6	166.4	1.580	371.4	585.9

**Table A-1(i): LM 3/8", with Masses, 3000 lb., SRS (Q=10),  
Log-Normal Statistical Features of Combined Normal & In-Plane, & Various Axis  
Groupings. Number of Samples = 45 Gumbel Factor = 0.9381**

Freq Hz	Arithmetic Mean		Log Mean nfyi	Standard Deviation	95th Percentile		Maximum		95th Percentile		Maximum	
	nfyi	nfyi			nfyi	nfyi	nfi	nfi	nfy	nfy	nfx	nfx
110	28	23	1.810	74	66	94	56	84	66	50	33	
124	29	25	1.801	78	74	95	55	91	74	49	33	
139	30	26	1.762	79	81	83	50	99	81	52	35	
156	33	28	1.734	82	90	72	50	108	90	54	38	
175	35	30	1.714	87	99	60	48	119	99	59	40	
197	39	34	1.720	99	109	60	48	138	109	68	45	
221	46	40	1.710	113	120	72	58	152	120	68	47	
248	51	44	1.750	131	132	88	75	162	132	71	50	
278	57	48	1.807	154	142	109	92	177	142	79	59	
313	63	54	1.814	173	157	110	95	203	157	87	69	
351	71	61	1.834	199	174	140	117	211	174	94	77	
394	79	66	1.854	222	189	166	127	221	189	108	87	
442	86	72	1.877	247	210	171	133	256	210	120	97	
496	98	82	1.888	284	228	194	146	272	228	129	107	
557	107	90	1.883	310	249	204	156	302	249	130	112	
625	116	98	1.852	327	271	219	182	330	271	148	123	
702	127	107	1.864	362	298	275	217	361	298	181	145	
787	156	132	1.861	444	320	349	277	354	320	228	177	
884	187	159	1.834	520	391	521	391	365	333	292	219	
992	229	191	1.919	685	475	558	475	376	346	378	286	
1114	281	226	2.055	923	607	767	607	433	390	542	407	
1250	324	258	2.122	1124	650	822	650	533	432	812	596	
1403	426	333	2.122	1449	1051	1535	1051	559	464	1221	966	
1575	549	406	2.245	1978	1537	2544	1537	600	480	1517	1367	
1768	675	486	2.360	2607	1849	2819	1849	588	488	1945	1733	
1984	689	527	2.199	2461	1625	2186	1625	620	472	1639	1458	
2227	765	618	2.012	2427	1448	1720	1448	547	442	1819	1713	
2500	1163	872	2.279	4372	2367	2693	2367	781	680	2436	2276	
2806	1432	1103	2.191	5115	2933	3314	2933	1079	959	3565	3214	
3150	1837	1450	2.085	6106	3847	4129	3847	1061	1016	3675	3333	
3536	2614	2076	2.058	8522	4898	6500	4898	1521	1457	4684	4485	
3969	3349	2849	1.833	9327	6319	7003	6319	2647	2144	6270	5268	
4454	4727	4379	1.502	9710	8674	10139	8674	4372	3685	7415	6255	
5000	5586	5252	1.435	10642	10967	12712	10967	6682	5417	7373	6419	
5612	5316	4946	1.484	10713	10591	12242	10591	7152	5744	7290	5800	
6300	4589	4157	1.595	10367	9401	10789	9401	5319	4558	7315	5821	
7071	4555	3938	1.732	11538	9648	16415	9648	4222	3474	9037	8117	
7637	4608	3794	1.871	12924	10210	21477	10210	3744	3230	10699	10157	
8909	5242	4357	1.841	14384	11570	23549	11570	4368	3695	12431	11749	
10000	5991	4784	1.972	18074	14280	26800	14280	3813	3258	17640	12885	

**Table A-2(a): OEA 3/8", Bare Panel, 7000 lb., SRS (Q=10), Log-Normal Statistical Features of Combined Normal & In-Plane, & Various Axis Groupings. Number of Samples = 11 Gumbel Factor = 0.8407**

Freq Hz	Arithmetic Mean nfyi	Log Mean nfyi	Standard Deviation	95th Percentile nfyi	Maximum nfyi	95th Percentile nfpf	Maximum nfpf	95th Percentile nfy	Maximum nfy	95th Percentile nfxz	Maximum nfxz
110	11	8	2.489	43	29	33	29	33	26	32	25
124	11	8	2.502	45	28	29	28	33	25	34	25
139	11	8	2.444	44	25	28	25	30	24	36	25
156	11	9	2.173	39	23	26	20	29	23	35	20
175	12	10	2.083	38	23	27	20	25	23	35	20
197	14	11	1.986	41	30	33	30	29	24	37	28
221	15	12	2.004	45	33	42	33	29	26	40	28
248	16	13	1.922	46	36	41	36	28	22	42	26
278	18	15	1.868	49	38	45	38	26	25	46	28
313	21	18	1.878	59	43	48	43	35	22	52	32
351	24	21	1.740	61	44	54	44	36	23	56	38
394	28	26	1.536	58	46	52	46	39	32	64	43
442	33	31	1.466	64	49	55	49	37	29	73	49
496	36	33	1.481	70	61	69	61	32	30	79	56
557	37	33	1.706	90	74	89	74	33	35	88	63
625	44	39	1.695	105	81	100	81	43	43	100	72
702	50	44	1.671	116	99	115	99	48	45	113	85
787	60	54	1.639	137	111	130	111	59	53	136	107
884	70	61	1.713	169	131	154	131	56	49	153	125
992	81	68	1.865	221	150	188	150	68	67	195	150
1114	100	86	1.790	258	203	239	203	76	78	264	199
1250	125	113	1.618	281	258	270	258	144	110	332	258
1403	168	147	1.716	407	451	447	451	205	155	472	451
1575	224	183	1.862	595	688	832	688	180	137	697	688
1768	279	216	2.027	822	937	1200	937	229	201	927	919
1984	299	252	1.808	773	722	988	722	260	219	817	722
2227	328	287	1.693	778	653	937	653	297	266	728	653
2500	378	331	1.700	905	733	879	733	322	325	762	727
2806	473	428	1.608	1053	943	1007	943	729	625	771	741
3150	497	470	1.397	885	1071	1099	1071	686	536	677	732
3536	464	435	1.433	860	912	1075	912	640	603	911	743
3969	543	503	1.464	1035	1296	1511	1296	703	628	901	1033
4454	660	621	1.413	1196	1405	1545	1405	1070	828	967	1008
5000	736	711	1.306	1179	1168	1268	1168	1193	970	897	812
5612	1020	971	1.391	1814	1844	1852	1844	1625	1341	1584	1697
6300	1204	1170	1.275	1854	1980	2183	1980	1600	1312	1644	1502
7071	1215	1140	1.437	2264	2229	3122	2229	1881	1741	1654	1776
7637	973	914	1.421	1777	1843	2692	1843	1196	1070	1586	1468
8909	1124	992	1.621	2477	2536	4354	2536	1233	1088	2127	2574
10000	972	864	1.622	2157	1992	3135	1992	930	904	1782	1959

**Table A-2(b): HiS 1/2", Bare Panel, 7000 lb., SRS (Q=10), Log-Normal Statistical Features of Combined Normal & In-Plane, & Various Axis Groupings. Number of Samples = 15 Gumbel Factor = 0.8688**

Freq Hz	Arithmetic Mean nfyi	Log Mean nfyi	Standard Deviation	95th Percentile nfyi	Maximum nfyi	95th Percentile nfip	Maximum nfip	95th Percentile nfy	Maximum nfy	95th Percentile nfzx	Maximum nfzx
110	9	5	2.929	35	26	29	26	5	6	31	29
124	9	6	2.686	32	29	29	29	5	7	33	32
139	11	7	2.610	39	44	37	44	7	7	40	36
156	14	9	2.566	48	64	50	64	10	9	53	58
175	17	11	2.520	58	63	60	63	15	14	65	80
197	17	13	2.166	50	61	54	61	19	17	56	71
221	16	12	2.009	42	44	44	44	15	19	44	51
248	16	12	2.112	46	60	46	60	15	15	47	56
278	20	14	2.330	63	79	65	79	15	14	68	83
313	20	15	2.205	60	64	54	64	15	15	59	79
351	20	16	2.017	54	50	50	50	16	17	46	54
394	24	20	1.927	62	73	64	73	19	19	66	76
442	25	23	1.613	53	53	52	53	28	31	52	59
496	31	28	1.539	60	71	65	71	41	42	59	66
557	32	30	1.480	59	57	58	57	42	44	54	65
625	33	30	1.557	66	71	69	71	38	34	60	61
702	34	30	1.658	72	82	76	82	34	31	60	58
787	41	37	1.585	83	90	89	90	54	50	67	64
884	54	50	1.476	99	117	107	117	81	94	76	67
992	70	63	1.581	141	172	141	172	113	143	111	100
1114	102	88	1.744	235	225	238	225	165	193	226	186
1250	106	92	1.792	255	213	248	213	159	165	261	214
1403	118	100	1.816	284	324	295	324	175	195	279	280
1575	155	129	1.822	370	598	445	598	207	265	376	554
1768	162	136	1.798	381	562	450	562	247	251	354	489
1984	151	132	1.699	335	471	359	471	242	259	291	452
2227	200	167	1.824	481	509	524	509	357	426	354	475
2500	324	260	1.978	861	778	870	772	605	778	569	659
2806	292	254	1.725	662	622	684	608	501	622	502	641
3150	280	260	1.483	519	617	581	617	433	467	443	551
3536	318	283	1.613	654	949	795	949	441	358	673	874
3969	322	292	1.544	625	951	787	951	460	392	603	812
4454	372	339	1.521	707	1044	878	1044	604	624	644	826
5000	515	472	1.518	982	1451	1209	1451	855	869	739	864
5612	558	517	1.488	1038	1200	1190	1200	974	935	837	972
6300	602	554	1.494	1120	1781	1326	1781	1009	874	824	844
7071	592	545	1.505	1116	1580	1393	1580	942	953	811	1025
7637	618	568	1.500	1157	1403	1469	1403	961	1051	963	1308
8909	763	696	1.515	1444	2477	1806	2477	1158	1454	1336	1975
10000	775	697	1.576	1550	2018	1930	2018	855	976	1415	1701

**Table A-2(c): G&H 3/8", Bare Panel, 7000 lb., SRS (Q=10), Log-Normal Statistical Features of Combined Normal & In-Plane, & Various Axis Groupings. Number of Samples = 44 Gumbel Factor = 0.9370**

1/6-Octave Freq Hz	X-Direction Lbf-Sec/ Inch	Y-Direction Lbf-Sec/ Inch	Z-Direction Lbf-Sec/ Inch
197	93.1	18.8	273.2
221	105	20.7	425.5
248	113.9	26.7	371.9
278	126.8	35.7	458.8
312	156.9	36.2	539.7
351	225.9	53.4	861.7
394	259.6	52.1	739.7
442	363.4	72.2	1157.6
496	534.8	87.7	1367.9
557	3009.6	84.8	5666.7
625	2570.9	98.1	3770.8
702	626.2	117.9	3254.8
787	302.6	139.1	1044.4
884	148.8	133.9	526.1
992	216.6	123.3	550.1
1114	96.6	150.2	221.6
1250	219.6	214.6	351.9
1402	286.8	303.6	248.8
1574	131.7	389.8	105.4
1767	107.1	370.4	373.7
1984	39.6	299.5	402.3
2227	13.6	264.2	154.9
2500	42.6	961.3	172.1
2806	85.8	1305.8	318
3149	103.4	1460.4	166.4
3535	106.8	734.4	874.7
3968	205.8	1098	574.8
4454	87.9	2718.1	292.3
5000	161.3	1318	505.2

**Table A-3(a): "Foot" Impedances for 3/8" Mount, X-Direction Tap.**

1/6-Octave Freq Hz	X-Direction Lbf-Sec/ Inch	Y-Direction Lbf-Sec/ Inch	Z-Direction Lbf-Sec/ Inch
197	401	17.8	260.2
221	545.5	22.6	312.2
248	522.4	27.1	306
278	549.9	33.7	411
312	913.7	32	588.8
351	904.9	49.8	710.1
394	670.9	52.4	694.9
442	975.3	76.7	916.8
496	1211.7	84.4	1884.2
557	1516.7	109.4	3478.1
625	2856.5	120.2	4143.2
702	3818.5	190.7	1063.6
787	4550.9	201.6	545.7
884	880.6	162.5	315.8
992	279.8	383.4	157.8
1114	601.2	243.5	470.1
1250	159.4	467.4	417.8
1402	210.2	600.4	298.7
1574	104.1	369	65.3
1767	694.3	524.5	180.1
1984	570.9	819.9	766.9
2227	222.6	189.7	498.1
2500	224.5	815.6	90.9
2806	289.1	543.5	690.4
3149	177.5	1017.5	288.5
3535	1526.2	332.7	229.3
3968	514	260.9	346.5
4454	496.1	508.9	364.5
5000	676.1	740.5	169.2

**Table A-3(b): "Foot" Impedances for 3/8" Mount, Z-Direction Tap.**

1/6-Octave Freq Hz	X-Direction Lbf-Sec Inch	Y-Direction Lbf-Sec Inch	Z-Direction Lbf-Sec Inch
197	230.1	10.6	231.6
221	689.3	9.4	244.9
248	1593.1	12.6	309.7
278	2283.2	17.8	467.7
312	1435	27.1	1021.9
351	1134.5	36.1	964.6
394	2144.7	73	795.4
442	652.1	15.7	339.2
496	3545.2	21.6	525.2
557	3275.5	41.6	1002.7
625	1542.9	34	952.5
702	1278.8	117.6	953.8
787	559.8	33.8	1500.8
884	447.1	29.7	1446.6
992	318.7	117.9	535
1114	719.1	68.9	365.7
1250	549.2	43.1	971.3
1402	3452.3	108.8	2301.2
1574	945	221	7246.7
1767	1691.6	82.2	1409.1
1984	588.4	119.3	749.5
2227	336.3	36.6	1050
2500	630.8	93.9	2467
2806	709.8	95.1	1137.7
3149	1279.8	119	1259.1
3535	613.1	86.5	518.8
3968	1031.4	59	768.2
4454	1931.2	83.2	2908.4
5000	1454	103	876.7

**Table A-3(c): "Foot" Impedances for 3/8" Mount, Y-Direction Tap.**

# REPORT DOCUMENTATION PAGE

*Form Approved*  
OMB No. 0704-0188

Public reporting burden for this collection of information is estimated to average 1 hour per response, including the time for reviewing instructions, searching existing data sources, gathering and maintaining the data needed, and completing and reviewing the collection of information. Send comments regarding this burden estimate or any other aspect of this collection of information, including suggestions for reducing this burden, to Washington Headquarters Services, Directorate for Information Operations and Reports, 1215 Jefferson Davis Highway, Suite 1204, Arlington, VA 22202-4302, and to the Office of Management and Budget, Paperwork Reduction Project (0704-0188), Washington, DC 20503.

<b>1. AGENCY USE ONLY (Leave blank)</b>		<b>2. REPORT DATE</b> December 1996	<b>3. REPORT TYPE AND DATES COVERED</b> Technical Memorandum	
<b>4. TITLE AND SUBTITLE</b> Comparison of Separation Shock for Explosive and Nonexplosive Release Actuators on a Small Spacecraft Panel			<b>5. FUNDING NUMBERS</b> WU 233-10-14-04	
<b>6. AUTHOR(S)</b> M. H. Lucy, R. D. Buehrle, and J. P. Woolley				
<b>7. PERFORMING ORGANIZATION NAME(S) AND ADDRESS(ES)</b> NASA Langley Research Center Hampton, VA 23681-0001			<b>8. PERFORMING ORGANIZATION REPORT NUMBER</b>	
<b>9. SPONSORING / MONITORING AGENCY NAME(S) AND ADDRESS(ES)</b> National Aeronautics and Space Administration Washington, DC 20546-0001			<b>10. SPONSORING / MONITORING AGENCY REPORT NUMBER</b> NASA TM-110257	
<b>11. SUPPLEMENTARY NOTES</b> Lucy and Buehrle: NASA Langley Research Center, Hampton, Virginia; and Woolley: Lockheed Martin, Sunnyvale, California				
<b>12a. DISTRIBUTION / AVAILABILITY STATEMENT</b> Unclassified-Unlimited Subject Categories 15, 18, 20, and 37  Availability: NASA CASI, 301-621-0390			<b>12b. DISTRIBUTION CODE</b>	
<b>13. ABSTRACT (Maximum 200 words)</b> Shock, safety, overall system costs, and emergence of new technologies have raised concerns regarding continued use of pyrotechnics on spacecraft. NASA Headquarters requested Langley Research Center (LaRC) study pyrotechnic alternatives using nonexplosive actuators (NEAs), and LaRC participated with Lockheed Martin Missile and Space Co. (LMMSC) in objectively evaluating applicability of some NEA mechanisms to reduce small spacecraft and booster separation event shock. Comparative tests were conducted on a structural simulator using five different separation nut mechanisms, three pyrotechnics from OEA Aerospace and Hi-Shear Technology and two NEAs from G & H Technology and LMMSC. Multiple actuations were performed with preloads up to 7,000 pounds, 7,000 being the standard. All devices except the LMMSC NEA rotary nut concept were available units with no added provisions to attenuate shock. Accelerometer measurements were recorded, reviewed, processed into Shock Response Spectra (SRS) and comparisons performed. For the standard preload, pyrotechnics were the most severe and the G & H NEA the least severe. Comparing all results, the LMMSC concept produced the lowest levels with preload limited to -4,200 pounds. Testing this concept over a range of 3,000 to 4,200 pounds indicated no effect on shock. This report presents data from these tests and the comparative results.				
<b>14. SUBJECT TERMS</b> spacecraft design, testing, and performance; spacecraft propulsion and power; mechanical engineering; launch vehicle and space vehicle			<b>15. NUMBER OF PAGES</b> 52	
			<b>16. PRICE CODE</b> A04	
<b>17. SECURITY CLASSIFICATION OF REPORT</b> Unclassified	<b>18. SECURITY CLASSIFICATION OF THIS PAGE</b> Unclassified	<b>19. SECURITY CLASSIFICATION OF ABSTRACT</b> Unclassified	<b>20. LIMITATION OF ABSTRACT</b> Unlimited	